RSC Applied Interfaces

ROYAL SOCIETY OF CHEMISTRY

REVIEW

View Article Online
View Journal | View Issue

Cite this: *RSC Appl. Interfaces*, 2026, 3, 26

From nanoparticle synthesis to assembly: DNA as a key structural material

Letian Han,† Yifan Yu,†* Peixin Li and Ye Tian *

Nanoparticles exhibit unique properties in optics, electricity, and other fields that differ from those of macroscale materials. Further assembling these functional nanoparticles may generate attractive physicochemical characteristics due to their collective properties. Different assembly structures result in diverse properties. Therefore, precise control over nanoparticle positioning remains a research hotspot, with numerous notable breakthroughs reported in the methodologies investigated. Recently, DNA emerged as a crucial structural material based on its exceptional programmability, addressability, and specific binding capabilities. Leveraging these excellent properties, DNA-functionalized nanoparticles can be accurately positioned at the nanoscale in accordance with predetermined spatial patterns. This capability facilitates the development of novel functionalities and significantly advances the programmable assembly of nanoparticles to a higher degree of sophistication. In this review, we present a systematic survey of the synthesis, functionalization, and assembly methodologies of nanoparticles, alongside an assessment of their current developmental status. Specifically, we systematically introduce several widely employed or potentially advantageous techniques for nanoparticle synthesis and summarize various categories of surface ligands that preserve the nanoparticle physicochemical properties. Based on the most representative DNA ligands, we present a discussion on the methodology and potential applications of DNA-mediated programmed assembly. Furthermore, we have outlined prospective directions and viable strategies for their future advancement.

Received 13th October 2025,
Accepted 1st December 2025

DOI: 10.1039/d5lf00313j

rsc.li/RSCApplInter

1. Introduction

The properties of materials undergo significant changes as the scale decreases from macro to micro, which is predominantly attributed to surface effects and quantum confinement.[1] Producing nanomaterials in the form of nano-sized particles is an effective approach to achieve their distinctive physical and chemical properties. These nanoparticles demonstrate considerable potential across various fields, including optics, medicine, catalysis, and energy storage. Moreover, their properties can be further precisely tailored through the controlled modification of their sizes, shapes, and compositions.[2,3] As a core objective of nanotechnology lies in precisely manipulating the arrangement of nanoparticles at the nanoscale to construct novel materials and devices with desired functions, these nanoparticles can serve as ideal "artificial atoms" for building functional materials through intrinsic, non-covalent interactions, such as hydrogen bonding, hydrophobic interactions, van der Waals forces, and electrostatic interactions. The entire assembling process is driven by thermodynamics, whereby free nanoparticles in high-energy states undergo transitions to form more stable periodic structures or clusters in low-energy states. The general assembly mode can be summarized into two types: (1) interface assembly, achieved by enriching and ordering nanoparticles at the interface between two immiscible phases;[4,5] (2) template-assisted assembly, guiding and constraining the spatial distribution of building blocks through pre-designed physical or chemical templates.[6,7] It is anticipated that utilizing the intrinsic properties of nanoparticles for assembly still presents significant potential for advancement in terms of thermodynamic control, dynamic stability, and structural programmability.

Recently, DNA-mediated assembly proposes a novel methodology for programmable structural fabrication and functional customization.[8] Watson–Crick base pairing endows DNA with powerful specific binding capabilities, thereby enabling researchers to encode the structural information of assemblies into DNA sequences and subsequently achieve precise construction of the target

College of Engineering and Applied Sciences, State Key Laboratory of Analytical Chemistry for Life Science, National Laboratory of Solid State Microstructures, Jiangsu Key Laboratory of Artificial Functional Materials, Chemistry and Biomedicine Innovation Center, Collaborative Innovation Center of Advanced Microstructures, Nanjing University, Nanjing 210023, China.
E-mail: dz20340025@smail.nju.edu.cn, ytian@nju.edu.cn
† These authors contributed equally to this work.

structure *via* specific hybridization. Utilizing this property of DNA molecules, the programmable assembly of nanoparticles can be achieved by attaching DNA strands or structures to their surfaces and further employing the specific interactions inherent in complementary base pairing. This approach advances the transformation of nanoparticles from "artificial atoms" into "intelligent atoms", endowing them with stronger spatial addressing and structural designability. To date, DNA-mediated assembly has facilitated the creation of thousands of structures and has further accomplished the inverse design of crystal structures *via* computational simulations.[9,10] Moreover, these DNA-mediated nanoparticle assemblies have exhibited tremendous potential in optics, catalysis, and other fields.[18,20,22,23] A systematic summary and organization of nanoparticle synthesis, ligand modification, assembly techniques, and applications can facilitate the identification of developmental challenges within the field and further promote the exploration of novel research directions and application opportunities (Fig. 1).

In this review, we first focus on the synthesis methodologies of nanoparticles, encompassing conventional chemical synthesis methods, green chemistry approaches with significant potential for further advancement, and DNA-mediated synthesis method for customizing complex shapes and components of nanoparticles. Based on the nanoparticle synthesis, the selection and use of ligands directly determine the operational contexts and foundational uses of these nanoparticles. Therefore, we summarized the modification methods of conventional organic and inorganic ligands, with particular emphasis on programmable DNA ligands that integrate nanoparticle stabilization with diverse collective functionalities. Furthermore, we conduct a comprehensive overview of the diverse assembly methodologies proposed within structure DNA nanotechnology, categorizing them based on DNA-molecule-mediated nanoparticle assembly and DNA-structure-mediated nanoparticle assembly. Additionally, we summarize the emerging functionalities and prospective applications that DNA-mediated nanoparticle assembly offers in the field such as catalysis, optics, and other fields. Indeed, over several decades of advancement, the synthesis, functionalization, and assembly of nanoparticles have achieved significant improvements; however, numerous challenges on methodologies and applications require further optimization. From the standpoint of chemical synthesis to device applications, we present prospective directions and potential developmental pathways for the advancement of colloidal particle-based devices.

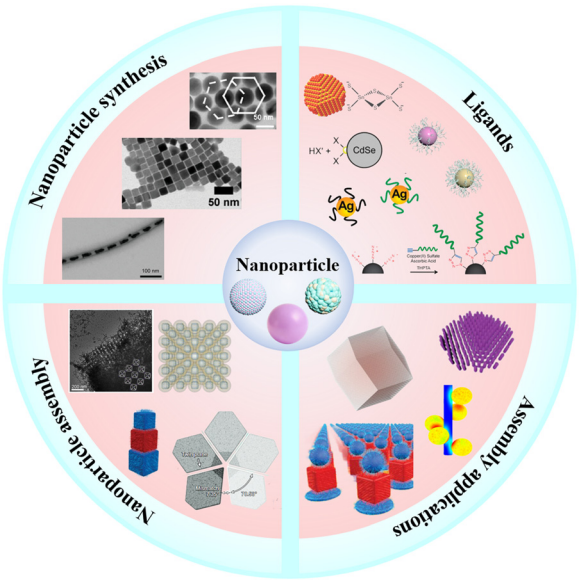

Fig. 1 The main content of the review. (Upper left) Synthesis of nanoparticles.[11–13] Copyright 2010, American Chemical Society. Copyright 2025, John Wiley and Sons. Copyright 2021, John Wiley and Sons. (Upper right) Ligands.[14–17] Copyright 2017, American Chemical Society. Copyright 2009, AAAS. Copyright 2007, American Chemical Society. Copyright 2010, American Chemical Society. (Lower left) Assembly of nanoparticles.[18–21] Copyright 2020, Springer Nature. Copyright 2018, AAAS. Copyright 2020, Springer Nature. Copyright 2023, Ye Tian *et al.* (Lower right) Assembly applications.[18,19,22,23] Copyright 2020, Springer Nature. Copyright 2022, American Chemical Society. Copyright 2018, the AAAS. Copyright 2022, Springer Nature.

2. Synthesis of particles

The synthetic methodologies for nanoparticles can be broadly categorized into two main pathways: "top-down" approach and "bottom-up" approach. Between them, the bottom-up synthesis method is more prevalent in nanoparticle fabrication owing to its high efficiency and cost-effectiveness. Therefore, this section primarily unfolds through the "bottom-up" strategy.

2.1 Classic methods for nanoparticle synthesis

In 1951, Turkevich *et al.* proposed an aqueous phase synthesis method based on the reduction of chloroauric acid by sodium citrate.[24] They successfully achieved controlled synthesis of spherical gold nanoparticles by modulating the concentration of sodium citrate, the reaction temperature, and the dilution of the solution (Fig. 2a). This Turkevich method has become one of the main methods for synthesizing gold nanoparticles since it was proposed. In addition to the Turkevich method, the Brust–Schiffrin method is another classical method for gold nanoparticle synthesis, which was proposed in 1994.[25] Brust *et al.* catalyzed the migration of chloroaurate from the aqueous phase to the toluene phase by tetraoctylammonium bromide phase transfer. Gold nuclei were then generated by reduction with sodium borohydride, and the surface was passivated *in situ* using alkyl mercaptans, thereby synthesizing size-controlled monodisperse gold nanoparticles functionalized with mercaptan derivatives. Compared to the Turkevich method, the Brust–Schiffrin method enables the synthesis of gold nanoparticles at smaller sizes. Moreover, the resulting gold nanoparticles exhibit superior dispersion and stability. The sodium citrate reduction method is also applicable to the synthesis of silver nanoparticles. In 1982, Meisel *et al.*

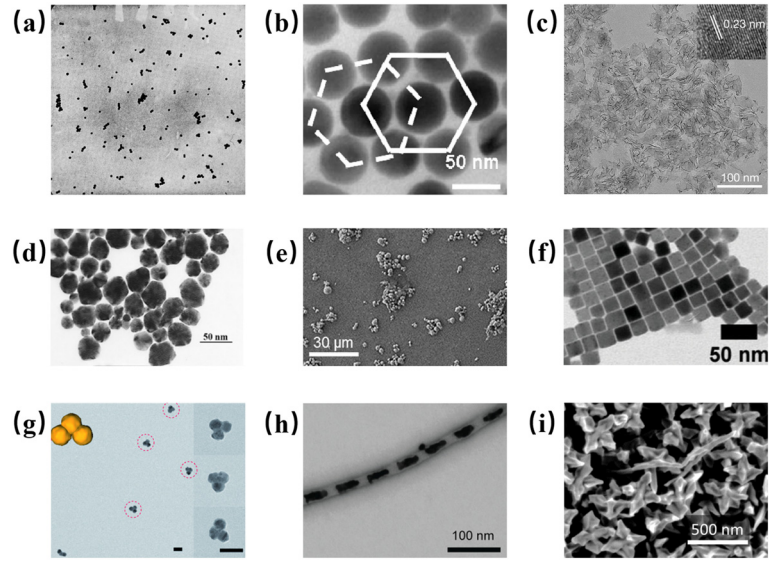

Fig. 2 (a–c) Classic methods for nanoparticle synthesis. (a) Synthesis of gold nanoparticles using the sodium citrate reduction method, magnification 50 000 diameters.[24] Copyright 1951, Royal Society of Chemistry. (b) TEM image of the silver nanospheres.[11] Copyright 2010, American Chemical Society. (c) TEM image of PdMo bimetallene.[31] Copyright 2019, Springer Nature. (d–f) Green methods for nanoparticle synthesis. (d) TEM image of produced gold nanoparticles by *F. oxysporum*.[32] Copyright 2019, Elsevier. (e) SEM image of *Cassia fistula*-mediated ZnO NPs.[33] Copyright 2020, Springer Nature. (f) TEM image of $CsPbI_3$ nanospheres.[12] Copyright 2025, John Wiley and Sons. (g and h) DNA-mediated methods for nanoparticle synthesis. (g) TEM image of the triangular trimer. Scale bar: 50 nm.[34] Copyright 2020, Royal Society of Chemistry. (h) DNA template growth.[13] Copyright 2021, John Wiley and Sons. (i) SEM image of chiral gold nanoparticles synthesized with A50 oligomers.[35] Copyright 2022, Springer Nature.

used this method to synthesize silver nanoparticles successfully.[26] However, the morphology and size of silver nanoparticles synthesized by this method were usually inhomogeneous. Xu's group proposed a new route which can synthesize uniform silver nanoparticles with an average diameter of 54 nm in high yield.[11] Within this strategy, polyethylene glycol (PEG) functioned dualistically as the solvent and reducing reagent, whereas polyvinylpyrrolidone (PVP) served the role of a capping agent. Owing to PVP as a capping agent, this method yields silver nanoparticles with more uniform sizes compared to the citric acid method (Fig. 2b).

In addition to single-component nanoparticles, multi-component nanoparticles are worthy of attention as well. Due to synergistic effects between metals, multi-metal nanoparticles composed of different metal elements demonstrate unique physical and chemical properties that are superior to those of single-metal nanoparticles in specific applications.[27] The co-reduction method is a simple method for synthesizing random alloy nanocrystals. Sun *et al.* used *tert*-butylamine borane as a reducing agent to co-reduce $Pd(acac)_2$ and precursors in oleyl amine solvent.[28] By adjusting the molar ratio of the precursors, they achieved linear control of the final components, and control of the particle size range was achieved through changing the morpholine borane injection temperature. In 2018, Ravishankar *et al.* employed a seed-mediated synthesis method.[29] The reaction was carried out at the liquid–liquid interface using microwave-assisted reduction technology. At the interface, ligand-guided reduction and alloying occurred, with Au nanowires serving as templates and ethylene glycol acting as a high-loss factor ($\tan\delta$ = 1.35) solvent to absorb microwave radiation. At 150 °C, the reduction of M (Cu, Pd, Pt) was triggered to achieve diffusion alloying. Generally, intermetallic compounds are synthesized using the direct annealing method. Gan's group prepared PtM_3 nanoparticles through organic-phase reduction, followed by carbon loading and stepwise annealing to form an ordered structure.[30] In 2019, Guo *et al.* synthesized the first sub-nanometer bimetallic graphene catalyst through the synergistic effect of strain, size, and alloying (Fig. 2c).[31] This catalyst was synthesised using a wet chemical one-pot method, with oleylamine as solvent, ascorbic acid to reduce $Pd(acac)_2$ and $Mo(CO)_6$, and low-temperature decomposition of the molybdenum precursor to achieve ultra-thin structures through synergistic kinetic control.

2.2 Green methods for nanoparticle synthesis

Conventional methods of nanoparticle synthesis suffer from high energy consumption and high cost, which is not friendly to the environment, while green synthesis methods synthesize nanoparticles using microorganisms or plant extracts, which is environmentally friendly and low energy consuming.[36]

In recent years, green synthetic methods have become a trend. In 2019, the Dolatabadi group proposed a biosynthetic method for the reduction of chloroauric acid without the

need for chemical reductants (Fig. 2d).[32] *Fusarium spinosum* culture supernatant can reduce chloroauric acid and synthesize gold nanoparticles under mild conditions. Generally, microbial synthesis of nanoparticles consumes more time, and the culture medium is challenging to maintain for long periods. In contrast, plant extract synthesis uses natural raw materials derived from plants, which are more efficient.[37] In 2017, Mehata and Jain investigated the effects of different conditions (such as temperature, pH value, time, and concentration) on the reduction of silver ions by biomolecules present in tulsi.[37] Furthermore, Aziz *et al.* used extracts from *Mikania cordata* leaves to synthesize silver nanoparticles and studied their antibacterial effects.[38]

Metal oxide nanoparticles are of pivotal importance in the biomedical domain. Zinc oxide (ZnO) nanoparticles continuously release zinc ions in aqueous medium which can penetrate cell membranes, disrupting bacterial enzyme systems and metabolic processes. Its antibacterial property has great potential in the treatment of diseases. Recently, Ramamurthy *et al.* studied the anti-inflammatory and antioxidant activities of ZnO nanoparticles synthesized by green tea and chamomile tea.[39] Dhanemozhi *et al.* also used green tea extract as a reducing agent and stabilizer, reacting it with zinc acetate solution at 80 °C to synthesize ZnO nanoparticles.[40] After drying and calcination, these formed a hexagonal wurtzite structure with an average particle size of 54.84 nm. In addition, Chen *et al.* synthesized ZnO nanoparticles using leaf extracts from *Cassia fistula* and *Melia azedarach*, and evaluated their antibacterial properties (Fig. 2e).[33] As a direct-bandgap semiconductor, perovskite exhibits exceptionally high light absorption efficiency, thereby bringing a multitude of advances to optoelectronic devices. Locardi *et al.* developed a green, recyclable solvent strategy for synthesizing cesium–lead halide perovskite nanoparticles as an alternative to traditional petroleum-based solvents (Fig. 2f).[12] They selected limonene, a naturally sourced solvent, and recovered it from reaction waste *via* vacuum distillation, which was then used in secondary synthesis to validate reproducibility. This marks the first successful use of limonene for the efficient and recyclable synthesis of perovskite nanoparticles.

2.3 DNA-mediated methods for nanoparticle synthesis

The properties of nanoparticles are closely related to their composition, size, and shape.[41] However, controlling the size and shape of nanoparticles remains a huge challenge. Conventional synthetic methods and green synthetic methods still find it difficult to achieve the customizable morphology design of nanoparticles. Recently, DNA nanotechnology has provided a novel approach for the synthesis of nanoparticles.

Different bases on DNA interact differently with nanoparticle surfaces. By exploiting this property, DNA molecules can regulate the growth and morphology of nanoparticles. Lu *et al.* demonstrated that DNA molecules can serve as programmable ligands to fine-tune the morphology of nanoparticles. They provided an in-depth study for the role of DNA molecules in this regulation.[42] The DNA growth mechanism was divided into two stages: shape formation and volume growth. DNA affects the growth of AuNPs by surface passivation and kinetic hindrance of Au deposition. In 2020, Sleiman *et al.* proposed an assemble, grow and lift-off (AGLO) strategy, utilizing two-dimensional DNA origami as a recyclable template to programmatically assemble gold nanoparticle seeds and control their merging into customized nanostructures (Fig. 2g).[34] AuNP seeds with surface-modified DNA capture chains were directedly assembled onto 16-helix bundle DNA origami templates. HEPES buffer was used as a mild reducing agent to reduce $HAuCl_4$, enabling Au^{3+} deposition onto the AuNP seed surfaces. High-molecular-mass PVP360 was employed as a surfactant to prevent random nucleation and promote complete merging of adjacent AuNPs. Gold nanoparticles were stripped from the DNA template *via* urea chain displacement, yielding specific structures. In addition, Seidel *et al.* established a modular DNA template platform that enables the controlled synthesis of multidimensional complex metal nanostructures, such as branched and ring-shaped structures, by programming the interactions between basic units like templates, caps, and connectors (Fig. 2h).[13] Specifically, Nam *et al.* discovered that adenine homopolymers can induce significant chiral optical responses in gold nanoparticles, and investigated the influence of structural parameters on chiral evolution (Fig. 2i).[35] By designing the length, base sequence, and spacing type of the DNA sequence, precise control of the chiral morphology and optical properties was achieved.

Furthermore, DNA-mediated approaches can be employed to synthesize multicomponent nanoparticles. Lu *et al.* reported the use of DNA sequences (A10, T10, C10, G10) as capping ligands to control the morphology of Pd–Au bimetallic nanoparticles seeded by palladium nanocubes.[43] The study revealed that distinct DNA sequences significantly influence metal atom deposition, diffusion, and surface energy reduction through their differential binding affinities to metal surfaces and precursors, thereby guiding the formation of four unique structures: T10 forms a cubic octahedral core framework, A10 yields a rhombic cubic octahedron, C10 generates a cubic octahedron, and G10 produces a core-shell structure with a rippled surface. A10's strong interaction with the gold precursor triggered a unique aggregation-growth mechanism: small nanocrystals first formed and then redeposited onto the seed surface. This study not only revealed the pivotal role of DNA sequences in controlling bimetallic nanoparticle morphology but also expanded the application potential of DNA in synthesizing complex multifunctional nanomaterials.

3. Ligands

In the synthesis of nanoparticles, ligands are the key molecules that regulate their morphology, stability, and functionality. The selection of ligands directly affects the dispersibility, surface chemistry, and application of nanoparticles.[44] Nanoparticles possess an extremely high specific surface area and surface energy. Thermodynamically, they exhibit a strong tendency to reduce surface energy by aggregating with one another. Once aggregated, the properties of nanoparticles may change. Ligand molecules commonly feature a polar head group coupled with a nonpolar tail.[14,45] The tail of the ligand can generate steric hindrance to prevent nanoparticle agglomeration.

3.1 Conventional ligands

Organic ligands are instrumental in governing both the morphological evolution and the stability of nanoparticles. The hybrid brushes formed by grafting two incompatible polymers onto the surface of nanoparticles can form Janus or multivalent structures through microscopic phase separation. Recently, Jason and Amalie systematically studied the effects of graft distribution uniformity, thermal fluctuations, nanoparticle size, graft density, polymer incompatibility, and solvent quality on the structure of mixed brushes through computational simulations, and evaluated the experimental feasibility of Janus phases and multivalent phases.[46] Hens *et al.* investigated the exchange behavior, distribution patterns, and stability mechanisms of linear and branched carboxylates in the ligand shell of CdSe QD by combining nuclear magnetic resonance experiments with molecular dynamics simulations (Fig. 3a).[14] Linear carboxylates could achieve a mixed ligand shell that covers the entire surface, while branched carboxylates were unable to match the high-density stacking of the (100) crystal plane.

Different from organic components, inorganic ligands possess simple structures and are more readily obtainable. In nanocrystalline devices, the use of organic-based ligands may form insulating barriers, thereby reducing charge transport efficiency. Talapin *et al.* adopted a metal chalcogenide molecular ligand strategy (Fig. 3b).[15] By replacing insulating organic ligands and converting them *in situ* to a conductive phase, they solved the charge transport bottleneck in colloidal nanocrystal devices. In addition, infrared absorption by organic ligands masks signals and limits long-wave detection. Heiss replaced organic ligands with K_3BiI_6 to avoid infrared absorption.[49]

3.2 DNA ligands

DNA can be considered an organic ligand; however, unlike conventional ligands, DNA molecules act as crucial stabilizing agents as well as essential components for practical applications. DNA can confer the ability for programmable assembly to nanoparticles, which is difficult to achieve with conventional ligands. In addition, the stability and biocompatibility of DNA also make it more biologically safe compared to traditional ligands.

The unique molecular recognition capabilities of DNA are frequently leveraged to control and direct the behavior of nanoparticles within solution. When modified onto the surface of nanoparticles, the nanoparticles repel each other due to electrostatic forces, enabling stable dispersion of the nanoparticles. In 1996, Mirkin and Alivisatos simultaneously published their research on the modification of gold nanoparticles.[47,50] Mirkin treated DNA oligonucleotides as programmable ligands and used gold–sulfur covalent bonds to modify gold nanoparticles with thiolated DNA single strands (Fig. 3c). In Alivisatos' work, thiol-modified DNA single strands were coupled with monomaleimido-gold particles. DNA not only provides surface anchoring and stable

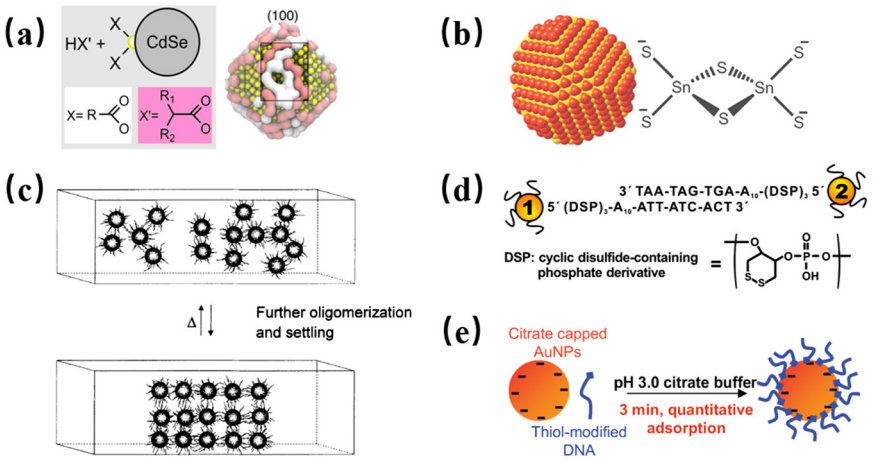

Fig. 3 (a and b) Conventional ligands. (a) Binding and packing in two-component colloidal QD ligand shells.[14] Copyright 2017, American Chemical Society. (b) Inorganic ligands, $Sn_2S_6^{4-}$ as a nanoparticle ligand.[15] Copyright 2009, AAAS. (c–e) DNA ligands. (c) Gold nanoparticles with thiolated DNA single strands.[47] Copyright 1996, Springer Nature. (d) Complementarity of DNA-modified nanoparticles.[17] Copyright 2007, American Chemical Society. (e) Low-pH method for DNA modification.[48] Copyright 2012, American Chemical Society.

dispersion but also enables specific connections between particles through base complementary recognition. In addition to the modification on the surface of gold nanoparticles, DNA molecules have also been investigated for their potential to be grafted onto other types of nanoparticles, thereby fully exploiting the functional coupling properties of diverse nanoparticles. In 2007, the Mirkin group designed a functionalized single-strand DNA that bound strongly to the surface of silver nanoparticles in order to improve the high salt stability of silver nanoparticles (Fig. 3d).[17] They constructed a DNA sequence containing a tricyclic disulfide group and utilized its multidentate ligand effect to enhance the binding force on the silver surface. This anchoring group significantly improved the stability and loading efficiency.

The salt aging method is a well-established technique for modifying DNA single strands on nanoparticle surfaces. However, this method usually requires a long modification cycle. In 2012, Liu's group reported low-pH for modifying gold nanoparticles, greatly reducing the time required for DNA modification.[48] They used a pH 3.0 citric acid buffer containing 30 mM Na^+ and then mixed the thiolated DNA with gold nanoparticles for only a few minutes to complete the modification (Fig. 3e). The DNA adsorption density increased by 30% at pH 3. Low pH can reduce charge repulsion by protonating DNA bases, thereby promoting the rapid adsorption. In 2017, Liu's group continued to develop a cryogenic method to rapidly modify high-density DNA.[51] Thiolated DNA was mixed with a solution of gold nanoparticles capped with citric acid. This mixture was frozen at −20 °C for several hours or only 2 minutes in dry ice. The DNA loading density of the cryogenic method is significantly higher than that of the salt aging method and the low pH method. During freezing, ice crystal growth repels AuNPs, DNA, and salt ions, forming localized high-concentration micro-pockets that accelerate the formation of Au–S bonds between thiolated DNA and the gold surface. In 2025, Wolfrum *et al.* summarized four DNA functionalization techniques: salt aging, pH-assisted, freeze-oriented, and microwave-assisted.[52] They analyzed the operational characteristics and applicability of each method and established a method performance mapping model covering different chain lengths.

In addition to the interaction between thiol groups and metal nanoparticles, azide–alkyne cycloaddition reactions were also employed for DNA modification of nanoparticles. The Mirkin group conducted research on the modification of iron oxide nanoparticles.[16] Azide groups were introduced onto the surface of iron oxide nanoparticles, and acetylene groups were grafted onto the ends of oligonucleotides. DNA modification on the surface of the nanoparticles was achieved through the azide–acetylene reaction. In 2020, they employed a similar approach to induce reaction between metal–organic framework nanoparticles bearing azide-terminated groups and DNA modified with diarylcyclooctyne-terminated groups, which successfully achieved DNA functionalization of the metal–organic framework.[18] Furthermore, the binding constant between streptavidin and biotin is exceptionally high. Based on this property, the Alivisatos group prepared DNA-modified quantum dots by directly conjugating biotinylated DNA to streptavidin-coated quantum dots.[53]

It is worth noting that a kind of ligands may not universally match all types of nanoparticles, and researchers need to continuously find ligands that are suitable for specific nanoparticles.[54] The number of ligands in current commercial ligand libraries is far smaller than the number of ligands that are theoretically possible. Traditional methods for finding the best ligands are inefficient. Zito and Infante unified the thermodynamic framework, constructed a large-scale ligand property database, and combined machine learning algorithms to predict the optimal ligand structure, which can greatly reduce the cost of experimental trial and error.[54] In the future, this method may help researchers find better ligands more efficiently.

4. Assembly of nanoparticles

Nanoparticles can be assembled to form new materials with specific structures and acquire new properties that differ from those of individual nanoparticles.[55–57] DNA, as a powerful structural material, enables programmable, addressable, and specific assembly of nanoparticles. DNA-mediated assembly relies on base-specific hybridization, which means it possesses a high programmability. By adjusting the length of DNA strands and the type and size of nanoparticles, nearly any desired spatial arrangement can be achieved. This technology for engineering precise superlattices has advanced rapidly over the past decades. It features distinct characteristics such as controllable composition, dynamic lattices, and inverse design. At present, there are two main strategies for DNA-mediated nanoparticle assembly. One strategy uses nanoparticles as templates, with DNA strands bound to their surfaces, enabling the nanoparticles to form directed interactions.[58,59] The other strategy is based on DNA strand assembly structures, which load nanoparticles for assembly. For the second strategy, depending on the structure of the DNA assembly, it is divided into DNA tile[60,61] and DNA origami.[8,62]

4.1 DNA strand-mediated assembly

4.1.1 Assembly of isotropic nanoparticles. In 1996, Mirkin *et al.* and Alivisatos *et al.* first independently reported their achievements in using DNA single strands to modify gold nanoparticles.[47,50] After modifying DNA strands onto gold nanoparticles, a third DNA strand was used to assemble the gold nanoparticles through pairing with the single-stranded DNA on the gold nanoparticles. This type of DNA–nanoparticle, capable of directing the assembly of crystal structures, was subsequently defined as spherical nucleic acid (SNA) by Chad Mirkin.[63] Although this structure plays a significant role in *in vitro* biological

detection[64,65] and intracellular detection,[66,67] this review primarily focuses on its role in mediating assembly and the functions of the assembled structures. Subsequently, researchers focused on the assembly properties of this DNA–nanoparticle structure. Progress ranged from nanoparticle aggregates in 1996 to the assembly of simple ordered lattices in 2008, followed by the construction of diverse lattices in 2011 and high-quality lattices in 2014. By merely leveraging complementary interactions between DNA single strands, diverse crystal structures could already be constructed.

For nanoparticles exhibiting external field responsiveness, the external field can be utilized as the primary driving force to guide the spatial arrangement of the nanoparticles. Markin *et al.* reported that Fe_3O_4 nanoparticles modified with complementary DNA formed a body-centered cubic lattice through DNA hybridization during slow cooling.[68] Upon application of an external magnetic field, magnetic dipole coupling induced anisotropic growth of the crystals along the magnetic field direction, resulting in a rod-like polycrystalline structure (Fig. 4a). In addition to magnetic field effects, Jiang *et al.*[69] proposed a new strategy for DNA–gold nanoparticle assembly driven by an alternating electric field. Parameters of the alternating electric field induced deformation of DNA chains, promoting reversible bond rearrangement and guiding the system from a locally minimum metastable state to a global minimum. This approach overcame the limitations of traditional thermal annealing methods in temperature-sensitive systems, enabling efficient and precise assembly of face-centered cubic crystals.

In addition to field-mediated assembly, researchers propose other DNA assembly strategies. By using azobenzene-modified DNA (azoDNA) as a bonding element, the hybridization state of DNA can be regulated by photoisomerization. Mirkin *et al.* assembled gold nanoparticles using azoDNA to form body-centered cubic and face-centered cubic superlattices (Fig. 4b).[70] Within the ΔT_m window, they achieved reversible cycles of crystal assembly and dissociation by switching between UV and visible light irradiation. In 2025, they proposed a new strategy for kinetic challenges in crystal growth. Formamide could competitively weaken hydrogen bonding between DNA bases, thereby controllably slowing crystal growth rates.[71] Formamide preferentially disrupted hydrogen bond networks in DNA flexible regions, enhancing long-range order through its "etching–regrowth" effect. At 15–20 wt% concentrations, the DNA re-stranding hysteresis region was significantly broadened, promoting the dissociation and recombination of undercoordinated particles. This allowed crystal growth to fully relax, forming thermodynamically stable truncated octahedral Wulff structures. Yi *et al.* introduced mismatched bases into the sticky ends of DNA as a new tool for regulating T_m (Fig. 4c).[72] Single base mismatches can reduce the melting temperature of PS microsphere assemblies.

In addition to the typical complementary base pairing model, the DNA structure exhibits other pairing patterns. For instance, guanine-enriched strands can reversibly reconfigure into G-quadruplexes in the presence of certain cations.[73] Assembling G-quadruplets on nanoparticle surfaces can regulate the dynamic aggregation/disaggregation process of nanoparticles.[74] Willner *et al.* achieved reversible aggregation and disaggregation of CdSe/ZnS QDs by utilizing potassium ion-stimulated G-quadruplets as bridging units within aggregates. Crown ether was able to induce G-quadruplex dissociation, accompanied by the depolymerization of CdSe/ZnS QDs. Through the continuous interaction between the system and K^+ ions/crown ether, the periodic formation and separation of QD aggregates were achieved.[75] Subsequently, they controlled this dynamic process using fuel DNA strands and endonucleases. They designed two types of QDs modified on separate DNA strands, each containing segments capable of forming G-quadruplexes. By introducing specific fuel DNA strands, a chain displacement reaction was triggered, releasing a DNA strand that acted as a "bridge". This bridge

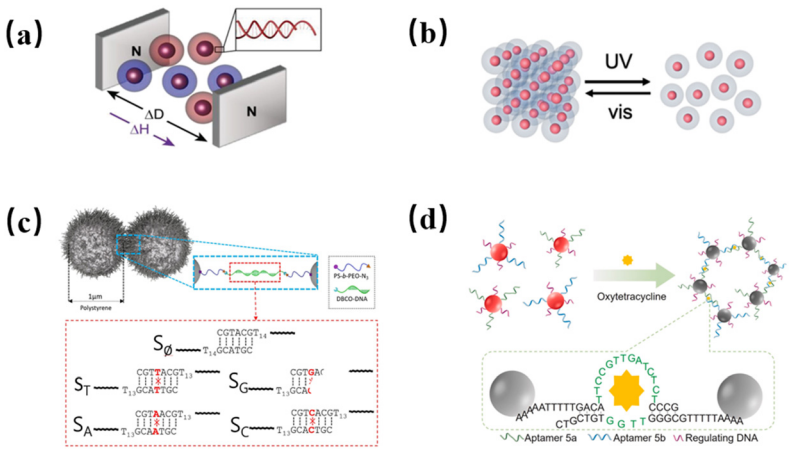

Fig. 4 Assembly of isotropic nanoparticles. (a) Assembly of nanoparticles in magnetic fields.[68] Copyright 2019, John Wiley and Sons. (b) Disconnection under ultraviolet light.[70] Copyright 2020, John Wiley and Sons. (c) Mismatch of some bases.[72] Copyright 2024, American Chemical Society. (d) Split adaptor-guided assembly.[80] Copyright 2025, Elsevier.

not only reversibly cross-linked the QDs into nanoaggregates but, more crucially, precisely guided the DNA on the QD surfaces to self-assemble into G-quadruplex structures at the aggregation interface. This DNA-mediated assembly was not static but dynamic and transient. Subsequently, endonucleases within the system acted as "dissipative" elements, degrading fuel by-products to reverse the DNA bridging structure. This led to the dissociation of aggregates and the disappearance of G-quadruplexes, which has the potential to construct dynamic lattices.[76]

Certain short oligonucleotides can bind to specific target molecules with high specificity and affinity; which are selected through systematic evolution of ligands by exponential enrichment (SELEX) and are recognized as DNA aptamers.[77] Splitting DNA aptamers yields split aptamers which can simultaneously bind to target molecules. In 2022, Liu *et al.* employed the SELEX method to screen for novel DNA aptamers targeting OTC. At least four distinct families of aptamer sequences were obtained, with the OTC5 sequence receiving focused investigation due to its high affinity and broad-spectrum activity against three tetracycline antibiotics.[78] Recently, they reported a non-thiolated SNA synthesized *via* thermal drying and investigated its functional characteristics and applications in the split adaptor (OTC5) mode. They discovered that high-density DNA modification inhibited binding to target molecules due to steric hindrance. To address this, they introduced short diluent chains to regulate probe density, successfully constructing a gold nanoparticle-based colorimetric sensor that achieved sensitive detection of oxytetracycline.[79] When target OTC was present, gold nanoparticles could spontaneously undergo self-assembly (Fig. 4d). Although current research on split aptamers focuses on molecular detection and sensor applications, their binding properties with target molecules also hold potential for nanoparticle assembly.

4.1.2 Assembly of anisotropic nanoparticles. As mentioned above, the morphology of nanoparticles has a significant influence on their properties. For isotropic nanoparticles, assembly techniques are well established. The assembly of anisotropic nanoparticles can generate novel properties, and anisotropic assemblies can form structures with ordered orientation. Therefore, researchers gradually turn their attention to the assembly of anisotropic nanoparticles.

In 2018, the Mirkin group utilized pores in a PMMA template to provide a confined environment, guiding anisotropic nanoparticle layer-by-layer assembly perpendicular to the substrate. By combining top-down lithography with bottom-up DNA-programmed assembly, large-area, periodic nanoparticle structures were fabricated on gold-plated silicon substrates (Fig. 5a).[19] DNA with locked nucleic acid-modified sticky ends precisely controlled nanoparticle interactions, spacing, and orientation. The oligonucleotide bonds connecting nanoparticles exhibited dynamic responsiveness, reversibly contracting or expanding in response to changes in polarity. This property enabled precise regulation of the distance between nanoparticles.

Chemical modification or sequence design of DNA ligands can regulate their binding strength, flexibility, and functionality.[72,81] In 2024, Mirkin *et al.* proposed an innovative oligoethylene glycol (OEG) flexible spacer strategy (Fig. 5b).[81] By inserting flexible OEG units between rigid DNA anchor chains and sticky ends, they achieved space-filling assembly of 10 types of polyhedra and even assembled a Penrose P1 quasicrystal with fivefold symmetry.

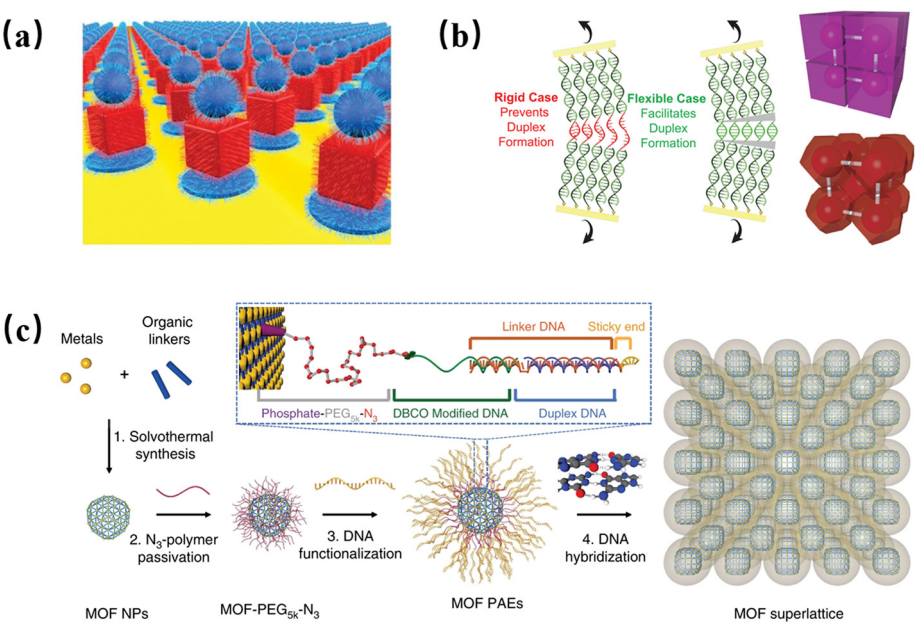

Fig. 5 Assembly of anisotropic nanoparticles. (a) Each unit cell of the NP superlattice consists of a gold surface, circular disk, and cube.[19] Copyright 2018, AAAS. (b) Rigid DNA strands and flexible DNA strands.[81] Copyright 2024, AAAS. (c) Crystallization engineering of MOF particles.[18] Copyright 2020, Springer Nature.

Subsequently, they optimized the DNA length and OEG unit number, achieving local five-coordinate and six-coordinate motifs.[82] They obtained millimeter-sized single-component colloidal tetragonal quasicrystals, solving the long-standing challenge of rational design and precise synthesis of colloidal quasicrystals. They subsequently passivated the metal–organic framework (MOF) particles by coating them with a layer of azide-modified PEG polymer, followed by DNA functionalization *via* copper-free click chemistry (Fig. 5c).[18] Spherical UiO-66 nanoparticles self-assembled into face-centered cubic and body-centered cubic structures *via* DNA complementarity.

For large-sized anisotropic nanoparticles, the conventional slow-cooling method is prone to falling into a kinetic trap, resulting in disordered or defect-rich structures.[83,84] The Mirkin group proposed a high-temperature isothermal growth (HTIG) strategy.[85] Cubic and rhombic dodecahedral gold nanoparticles were modified with short DNA strands to maintain nanoparticle anisotropy and restrict ligand degrees of freedom. During assembly, the system temperature was maintained above the DNA single-strand dissociation temperature but below the crystal melting point. This allowed unbound nanoparticles to remain dynamically free, promoting their deposition onto ordered crystal nuclei.

Employing novel DNA single-strand-mediated assembly methods, researchers are dedicated to assembling superlattices with original topological structures that were previously difficult to achieve. Colloidal superstructures have great application potential in porous materials, optical materials, and functional materials.[86,87] Weck *et al.* utilized DNA-modified double-patch colloidal particles to achieve the programmed assembly of two-dimensional open, close-packed colloidal superstructures such as Kagome and honeycomb by synergistically controlling temperature, depletion agent concentration, and patch geometric matching.[88] The Mirkin group achieved the construction of the open lattice based on the complementary contact model (CCM).[89] Directional DNA bonding drove nanoparticles to form maximized face-to-face interactions with the substrate or adjacent nanoparticles. The substrate was functionalized with A-type DNA. B-type PAEs in gold nanoparticles were bound to the substrate, and A-type PAEs were then assembled. By selecting the shape of the nanoparticles and annealing conditions, the open lattice could be customized. In 2024, they broke through the limitations of CCM in traditional DNA-mediated assembly and solved the problem of non-space-filling shape nanoparticles being difficult to form low-symmetry superlattices.[90] Long-chain DNA and low aspect ratio double cones were assembled to form complex rhombohedral supercells, and for the first time, twisted Kagome superlattices were achieved through partial face alignment. Additionally, they successfully synthesized 12 types of open-channel superlattices employing hollow nanoparticles by regulating DNA flexibility to drive crystallization through slow cooling.[91] DNA-modified gold nanoparticles precisely occupied the alternating pores within the superlattices.

4.2 DNA tile-mediated assembly

Although DNA single strands demonstrate remarkable nanoparticle assembly capabilities, the outcomes of this strategy may vary for nanoparticles of different sizes, shapes, and compositions. Assembly of gold nanoparticles modified with single strands typically yields face-centered cubic and body-centered cubic structures, while achieving low-dense-packing structures or some clusters remains challenging. After decades of development in DNA single-strand-mediated nanoparticle assembly, researchers turned their attention to a DNA-structure-mediated assembly technique, which offers greater programmability and design flexibility. By designing DNA structures, this approach provides a nanoparticle assembly platform capable of achieving high precision and high complexity.

DNA tiles, as building blocks, can be systematically edited and engineered to assemble into structures through interactions.[61,92] In 1998, Seeman reported a DNA double-crossover (DX) tile structure.[93] Using this structure, three two-dimensional lattices with two distinct topological configurations were assembled. The Ke group designed a DNA DX tile featuring cohesive junctions on both sides.[94] These tiles were first assembled into one-dimensional DNA bundles. Subsequently, these DNA DX tiles and DNA bundles were used to construct three-dimensional structures which are capable of precisely assembling gold nanoparticles. DNA tiles possess programmable directional interactions that enable the assembly of targeted structures.[60] In 2023, Zhang *et al.* designed single-layer, double-layer, and triple-layer T-shaped crossover (TC) tiles, introducing T-shaped junctions into the antiparallel double-crossover (AX) cross-structure to form a vertical third arm.[60] This configuration maintained rigidity while adding an orthogonally coupled direction. In 2024, Zhang *et al.* designed a DNAzyme circuit-based catalytic assembly method for gold nanoparticles.[95] Hairpin structures containing DNAzyme cleavage sites were modified onto the gold nanoparticles' surface. In the initial state, assembly activity was inhibited by a pre-protective domain. Upon DNAzyme addition, cleavage of the hairpin loop exposed hidden sticky ends, activating the gold nanoparticles' binding site. There were three types of logical operations. In the YES gate, a single input DNAzyme cleaved the H1 hairpin on the 15-nm gold nanoparticle surface. In the AND gate, dual-input DNAzymes cleaved the hairpins on both 15-nm and 5-nm gold nanoparticles. In the OR gate, a single input cleaved the dual-site H3 hairpin on the 15-nm gold nanoparticle surface.

4.3 DNA origami-mediated assembly

Existing research indicates that DNA tiles have limited nanoparticle loading capacity, posing challenges for the assembly of specific structural nanoparticles.[96] Furthermore, DNA tile-mediated assembly still fails to achieve decoupling between the final structure and the intrinsic properties of the

nanoparticles themselves. In contrast, DNA origami structures allow for the construction of a specific framework where incorporating different nanoparticles does not alter the final structure. This also opens up possibilities for inverse engineering of the structure.

4.3.1 Nanoparticles as DNA origami linkers. The researchers initially attempted to position nanoparticles at the junctions of DNA origami structures, using the nanoparticles as linkers.

Gang *et al.* proposed a programmable assembly platform based on an octahedral DNA origami framework for constructing predefined three-dimensional nanoparticle clusters and low-dimensional arrays. By modifying vertex DNA sequences, the binding positions of different nanoparticles were controlled. By attaching particles of varying sizes to symmetrical sites, they successfully constructed asymmetric structures. These structures exhibited significant circular dichroism responses, enabling the design of chiral optical structures (Fig. 6a).[97] Subsequently, they proposed a method for assembling three-dimensional lattices using DNA-linked nanoparticles. This strategy precisely controls the topological connections between particles by designing the geometric shape of the framework, enabling the assembly of identical particles into distinct crystal structures. They designed five DNA origami polyhedral frameworks and connected gold nanoparticles at the framework vertices *via* DNA strands. Different origami structures successfully guided the nanoparticles to form specific crystal structures.[98] In 2022, Tian *et al.* proposed a two-stage assembly method inspired by atomic molecular systems (Fig. 6b).[99] They designed a tetrahedral DNA origami framework with a hexagonal helix bundle structure, whose vertices extend single-stranded DNA for connecting external spherical nanoparticles and internal extensions extend capture chains to position internal nanoparticles. This enabled the positioning of gold nanoparticles to construct single-particle clusters, four-particle clusters, and five-particle clusters. By altering the number of nanoparticles within clusters, crystal lattices such as face-centered cubic and diamond were programmed.

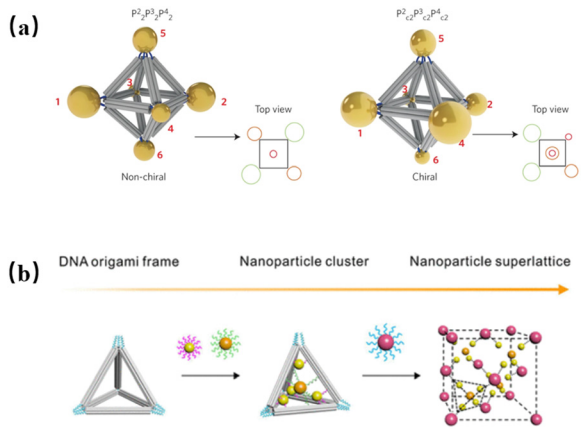

Fig. 6 Nanoparticles as DNA origami linkers. (a) Non-chiral and chiral nanoparticle clusters assembled on an octahedron frame.[97] Copyright 2015, Springer Nature. (b) Two-stage assembly of nanoparticle superlattices.[99] Copyright 2022, American Chemical Society.

4.3.2 Nanoparticles as cargo encaged in DNA origami. Using nanoparticles as linkers for DNA origami assemblies, the structure of the assembly still failed to achieve complete decoupling from the nanoparticles. Consequently, researchers conceived the idea of employing DNA origami as a carrier to mediate nanoparticle assembly, which significantly enhanced the programmability of the assembly.

Tian's group encapsulated gold nanoparticles within a single octahedral DNA origami framework (DOF) as a carrier. By modulating Mg^{2+} concentration in the environment as a conformational factor, they achieved programmable control over the crystal structure and morphology (Fig. 7a).[21] Furthermore, a phase diagram of the gold nanoparticle lattice was established, with Mg^{2+} strength and DOF monomer concentration as variables. Additionally, heterocrystalline structures and quintuple twins were discovered. In addition to the effect of magnesium salts on crystal formation, they also investigated the influence of externally added catalysts on the assembly process. In 2025, Yu *et al.* introduced urea to compete for hydrogen bonds between DNA base pairs, thereby weakening the inter-unit bonding forces in origami structures and promoting reorientation (Fig. 7b).[100] This approach achieved rapid room-temperature synthesis of DNA origami single crystals for the first time. By quantifying the relationship between urea concentration and temperature *via* phase diagrams, inverse engineering could be performed to tailor conditions to specific objectives. Furthermore, incorporating C-quadruplex structures confers pH responsiveness to the assembly. Tian *et al.* introduced i-motif sequences as dynamic linkers within origami structures. Under acidic conditions, the i-motif sequences folded into C-quadruplex structures, reverting to extended single strands under alkaline conditions. This enabled the directed reprogramming of the symmetry of three-dimensional DNA lattices in response to pH changes.[101]

Traditional DNA origami crystals rely on long, flexible single-stranded DNA to connect adjacent units, resulting in poor environmental stability of the crystals. Tian's group proposed a rigid DNA rod-bridged co-crystallization strategy (Fig. 7c).[102] By abandoning flexible long ssDNA linkers and instead employing rigid DNA structure quadruple helix bundles (4DH) and hexahelix bundles (6HB) to bridge octahedral DNA origami nanoscale frameworks loaded with gold nanoparticles, they constructed a three-dimensional simple cubic superlattice whose environmental stability was significantly enhanced. Through innovations in assembly methods, DNA origami technology further advanced in terms of the complexity and diversity of assembled structures. In terms of assembly strategy, hierarchical assembly enables the realization of more complex structures. Tian *et al.* proposed the concept of material voxels.[20] By constructing a DNA material voxel platform, they utilized DNA polyhedral frameworks as fundamental units, with vertices pre-

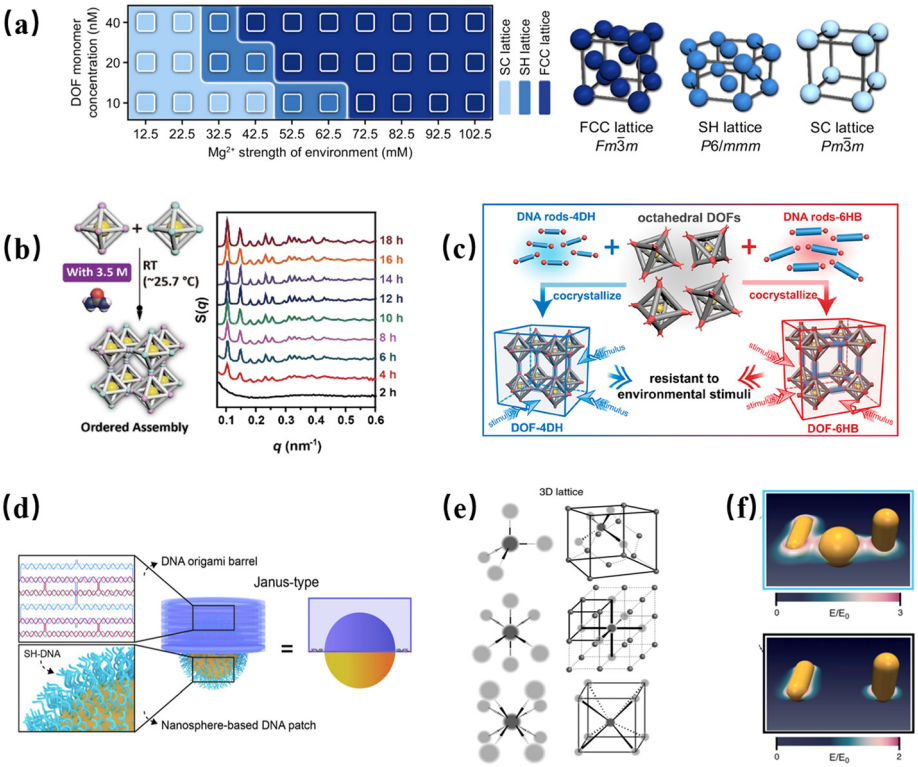

Fig. 7 (a) Lattice phase diagram of gold nanoparticles.[21] Copyright 2023, Ye Tian *et al.* (b) Room-temperature urea-catalyzed assembly and small-angle X-ray scattering.[100] Copyright 2025, the Royal Society of Chemistry. (c) DNA rods enhance structural rigidity.[102] Copyright 2021, American Chemical Society. (d) DNA buckets construct plaques on nanoparticle surfaces.[103] Copyright 2025, John Wiley and Sons. (e) Material voxel-constructed lattice.[20] Copyright 2020, Springer Nature. (f) Electric near-field intensity for NR–NS–NR and NR–NR.[104] Copyright 2021, Springer Nature.

programmed with complementary DNA sequences to confer controllable valence states. Within these DNA frameworks, they encapsulated inorganic nanoparticles, gold nanoparticles and QDs, alongside biomolecules streptavidin and enzymes, to build three-dimensional ordered structures with specialized functions (Fig. 7e). Ding's group proposed a hierarchical assembly strategy based on covalently bonded flexible branched DNA structures.[105] This architecture was synthesized *via* copper-free click chemistry, where azide-functionalized di-pentaerythritol cores were covalently linked to dibenzocyclooctyne-modified DNA oligonucleotides, overcoming the rigidity limitations of conventional DNA linkers. Pre-programmed capture chains at assembly vertices, edges, and centers enabled precise arrangement of diverse gold nanoparticles through DNA hybridization.

Innovations in connection methods and bonding techniques can enable enhanced precision in assembly structures. In 2025, Yao *et al.* employed the rigid framework of DNA origami buckets as a geometric constraint template to achieve region-specific patterning on gold nanoparticle surfaces through selective removal of protective layers (Fig. 7d).[103] The patterned nanoparticles then formed long-range ordered diamond superlattice structures *via* DNA-mediated directed interactions. Through the design of DNA origami, control over anisotropic structures and morphologies can be achieved. Liedl *et al.* designed a 100 nm DNA origami structure with two gold nanorods (NRs) anchored at its ends, spaced 62 nm apart and arranged in a 90° twisted L-shaped chiral configuration.[104] A 40 nm gold nanosphere (NS) was introduced as a propagating particle, positioned between the two rods to form an NR–NS–NR trimer (Fig. 7f). Compared to the NR–NR structure, the NR–NS–NR configuration exhibited a 3.5-fold enhancement in circular dichroism (CD) signal intensity. Wang's group employed cross-shaped DNA origami as an assembly scaffold to hybridize and immobilize anisotropic gold nanorods functionalized with DNA.[106] The four edges of the framework were modified with flat ends, where GC base pairs provided strong stacking interactions and AT base pairs provided weak stacking interactions. By dual-parameter regulation of ion concentration and DNA stacking strength, precise design of the AuNR array configuration was achieved. Low-symmetry DNA origami structures struggle to form ordered crystals *via* non-specific ligation. Tian's group achieved two highly ordered superlattices by employing multiple annealing cycles and increasing ligation site stiffness.[107] Enhancing ligation rigidity forced monomers to align geometrically. This work overcame traditional dependence on complex designs for crystallization, offering a simplified design pathway for anisotropic nanoparticle crystallization.

4.3.3 Inverse design assembly. As DNA origami-mediated assembly is becoming increasingly sophisticated, research

methodologies are shifting from trial-and-error design to goal-oriented intelligent design, revealing a trend toward inverse engineering.[108,109] The key to inverse design lies in first formalizing the adjacency relationships and pairing rules of the target lattice. Then, algorithms search within the combinatorial explosion of the design space for feasible solutions that satisfy hard constraints while avoiding dynamic traps and competitive phases, thereby preventing failures caused by common misstacking errors inherent in trial-and-error approaches. In 2024, Liu *et al.* established a comprehensive platform integrating computational design, multiscale simulation, and experimental validation.[9] They mapped the reverse design problem onto a Boolean satisfiability problem (SAT). This approach employs an interactive design process involving positive and negative constraints. The positive constraints ensure that the bonding relationships required for the target lattice can be simultaneously satisfied. Negative constraints are derived from numerical simulations of the assembly process using a coarse-grained tile particle model. Non-target competing structures identified in the simulation results are fed back as additional negative constraints to the optimization solver, thereby eliminating these competing states. By iterating this feedback loop, a solution for the target structure is ultimately obtained. They used SAT to demonstrate the infeasibility of single/dual-species schemes, establishing that at least four species are required and must be fully saturated to 24 colors to suppress traps. Subsequently, they validated this in patch-particle and oxDNA multiscale models, mapping solutions to icosahedral/octahedral origami structures. Finally, SAXS/SEM confirmed the realization of three-dimensional pyrochlore superlattices.

Kumar *et al.* investigated the self-assembly behavior of DNA origami octahedra with directional interactions through a combined approach of theoretical calculations, Monte Carlo simulations, and experiments.[110] The study revealed that altering the relative strength of vertex interactions leads to the formation of three distinct three-dimensional assembly morphologies. This theoretical model successfully predicted the phase diagram of morphological transitions. Rogers *et al.* proposed an inverse-design algorithm based on the symmetry of the two-dimensional wallpaper group.[111] By specifying unit cell parameters and symmetry operations, they derived the specific interaction matrix between particles using the four permitted rotational symmetries. Triangular primitives with 50 nm edges were fabricated *via* DNA origami, featuring sticky ends for orthogonal assembly. A gold nanoparticle superlattice comprising 12 components with a periodicity of 300 nm was successfully assembled. Gang *et al.* established an inverse-design framework based on DNA programmable bonds, guiding nanoparticle assembly into hierarchical three-dimensional structures by compressing mediator information through symmetry.[10] They achieved four representative systems in experiments. A key finding was that information minimization enhances crystal quality by reducing entropy penalties and optimizing growth kinetics. This strategy provided a universal design approach for multiscale functional nanomaterials. To address the bottleneck of design information overload in constructing complex three-dimensional nanostructures, they proposed the symmetry mapping algorithm MOSES.[112] This approach compressed design information through hierarchical equivalence classification, categorizing different structures into equivalent groups. By dynamically adjusting specificity through proportional thresholds, it balanced design complexity with assembly accuracy.

5. Applications of nanoparticle assemblies

The assembly of nanoparticles, as a versatile and highly efficient technique, enables the creation of structures with diverse functionalities.[113] DNA-mediated nanoparticle assembly structures exhibit unique properties, demonstrating exciting potential in the fields of catalysis, optics, and other fields.

5.1 Catalysis

Catalytic performance can be optimized by adjusting the composition and positioning of metal nanoparticles.[114] Mirkin *et al.* assembled a body-centered cubic superlattice of gold nanoparticles *via* DNA-mediated assembly.[115] The structure was immobilized by silica encapsulation and calcined at high temperatures to expose catalytic sites on the nanoparticles. The calcined superlattice retains its ordered structure with a surface area of 210 m^2 g^{-1}. They demonstrated the catalytic capability of the gold nanoparticle-loaded superlattice for alcohol oxidation. In 2020, Mirkin *et al.* achieved DNA-programmed superlattice assembly of MOF nanoparticles.[18] Nanorod PCN-222 was able to self-assemble respectively into 2D hexagonal and 2D square lattices *via* self-complementary or complementary DNA. This 2D superlattice of PCN-222 nanorods was available for the photooxidation of 2-chloroethyl ethyl sulfide. Structurally, nanoscale MOF particles accelerated substrate diffusion, while the 2D architecture enhanced light trapping capacity and penetration depth. Performance-wise, the superlattice exhibited significantly higher catalytic efficiency

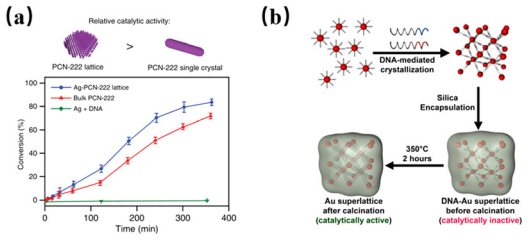

Fig. 8 (a) The photocatalytic activity of the 2D PCN-222 nanorod superlattices is examined.[18] Copyright 2020, Springer Nature. (b) Synthesis of catalytically active DNA–nanoparticle superlattices.[116] Copyright 2015, American Chemical Society.

than bulk PCN-222 single crystals, with conversion rates increased by approximately 30% (Fig. 8a).

By assembling nanoparticles into specific ordered structures *via* DNA, solid-state catalytic networks can potentially be formed to enhance catalytic performance. However, when numerous DNA strands are chemically bonded to nanoparticles, catalytic activity may decrease. Mirkin's group reported a method using silica coating and calcination to prepare gold nanoparticle superlattices suitable for catalysis (Fig. 8b).[115] First, they assembled a body-centered cubic gold nanoparticle superlattice and stabilized its structure by coating it with silica. Subsequently, they calcined the structure at 350 °C in air for 2 hours to remove the DNA, creating through-pores and exposing the gold surface. After calcination, the gold nanoparticle lattice structure remained ordered. Finally, the activity and structural stability were validated in aerobic alcohol oxidation, demonstrating the practical application of DNA-mediated assemblies in the field of catalysis.

DNA can precisely regulate the properties of nanozymes through adsorbing, conformational changes, sequence design, and interactions with substrates. The Yigit group investigated the regulation of peroxidase-like activity by adsorbing single-stranded DNA onto the surface of AuNPs. Following DNA adsorption, the catalytic activity of AuNPs initially exhibited a slight delay and was enhanced significantly by up to 2.5 times in the later stages of the reaction. Furthermore, they investigated the regulatory effects of DNA sequence, length, and base type on peroxidase activity.[117] The Zhang group investigated the regulatory effects of four DNA structures, single-stranded DNA (ssDNA), double-stranded DNA (dsDNA), hairpin DNA (H-DNA), and long dsDNA from hybridization chain reaction (HCR) products, on the peroxidase-like activity of two representative nanozymes Fe_3O_4NPs and AuNPs. HCR product-modified nanoparticles exhibited the highest catalytic enhancement effect.[118] In 2023, Yang *et al.* investigated the regulation of peroxidase-like activity in platinum nanozymes using different DNA sequences (A10, T10, C10, G10) as templates, with T10 exhibiting the strongest activity. Subsequently, they constructed a sensor array based on four types of PtNPs for distinguishing multiple antioxidants.[119]

Bimetallic nanozymes can combine the advantages of two metal nanoparticles. In 2024, the Zhang group employed four homologous oligonucleotides (A10, T10, C10, G10) as capping ligands to regulate the *in situ* growth of PtNPs on AuNRs, thereby constructing Pt–Au bimetallic nanozymes.[120] Among these, the AuNRs/A10/PtNPs structure exhibited the highest activity. Furthermore, they constructed a colorimetric sensor array based on four DNA-encoded nanozymes to distinguish five biological thiols and differentiate normal cells from tumor cells. Unlike AuNRs, Lu *et al.* employed gold double cones as substrates to mediate PtNP growth *via* the T15 sequence, constructing an Au/T15/Pt bimetallic nanozyme. This nanozyme was then utilized to develop a colorimetric sensor for detecting ascorbic acid, alkaline phosphatase and its inhibitors.[121] The construction of two-component nanozymes mediated by DNA enables synergistic integration of their respective characteristics. By leveraging DNA assembly techniques, researchers may design the assembly of diverse nanozymes to achieve more complex catalytic processes. Furthermore, combining DNA origami structures with nanozymes may enable the construction of miniature catalytic devices.

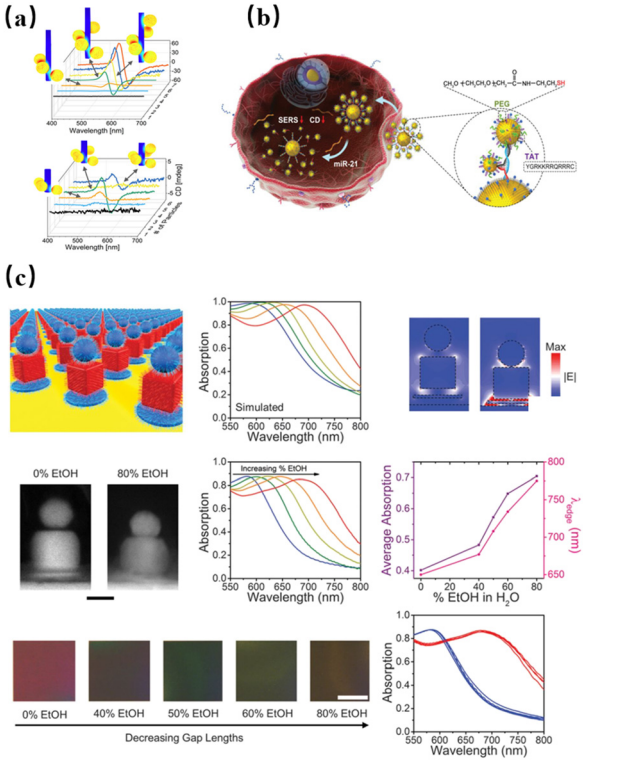

Fig. 9 (a) CD spectra of gold nanoparticle helical structures.[22] Copyright 2022, American Chemical Society. (b) Schematic representation of Y-DNA-driven construction of Au NP chiral $C_{30}S_5S_{10}$ NSs with enhanced CD and SERS signals. Copyright 2020, John Wiley and Sons. (c) Reconfigurable optical properties. Scale bar, 50 nm.[19] Copyright 2018, AAAS.

5.2 Optics

DNA assembly holds immense potential for the programmable and precisely engineered design of nanoscale structures within plasma.[122] The optical response of plasmonic nanostructures lies within the visible light spectrum, making them ideal model systems for studying chiral optical activity. Liedl *et al.* precisely assembled two types of gold nanoparticle helical structures using DNA origami technology (Fig. 9a).[22] The three-particle structure exhibited anomalous CD signals, with experiments revealing a distinct dip–peak CD response in the planar configuration which contradicted conventional symmetry theories. Electromagnetic simulations revealed that the dielectric effects of the DNA scaffold break symmetry, with DNA cylinders tilted through the particle plane inducing overall

structural chirality. By precisely assembling plasmonic helices *via* DNA origami, the study clarified that the origin of the chiral CD signal depends not only on geometric configuration but is primarily governed by metal–dielectric coupling.

Traditional nonlinear optical materials rely on the inherent non-centrosymmetry of crystals to generate second harmonic generation (SHG). However, plasmonic metasurfaces, constrained by planar structures and low packing density, have yet to achieve controllable SHG through bottom-up construction of three-dimensional plasmonic metamaterials. The Mirkin group assembled gold nano octahedrons *via* DNA programming to modulate superlattice symmetry, precisely controlling the symmetry by adjusting surface DNA density on the gold nano octahedrons.[123] The crystal generated a 450–490 nm SHG signal upon excitation at 900–980 nm, achieving the first bottom-up synthesis of plasmonic superlattices with tunable SHG properties.

DNA structures can assemble surface-enhanced Raman scattering (SERS) hotspots with strong field enhancement effects and precisely control the distribution of hotspots.[124] The Kuang group assembled a gold nanoparticle satellite structure by modifying three distinct sizes of gold nanoparticles with a Y-shaped DNA. This structure established a dual-signal sensing platform capable of highly sensitive and specific detection of miRNAs in living cell environments (Fig. 9b).[125] Furthermore, Bold *et al.* designed a DNA origami-based nanofork antenna structure for the precise assembly of gold or silver nanoparticle dimers, forming tunable nanogaps (as small as 1.17 nm) to achieve SERS detection at the single-molecule level.[126] In 2022, Chao *et al.* proposed a DNA origami-based "pattern recognition" strategy to assemble gold nanocubes into plasmonic gap structures with distinct geometric configurations. This approach enabled precise control over the shape and position of nanogaps, facilitating the construction of plasmonic structures with diverse geometries, which significantly enhanced the intensity and tunability of SERS signals.[127]

G-quadruplex-mediated assembly can regulate the dynamic aggregation/disaggregation process of nanoparticles, thereby forming nanoparticle assemblies with switchable optical properties. In 2021, the Willner group designed a dissipative reaction network driven by DNA and enzymes, enabling the dynamic, reversible assembly and disassembly of QDs based on G-quadruplexes. This dynamic assembly process directly translated into observable optical functional outputs: in the aggregated state, the G-quadruplex-bound heme-containing DNAzyme catalyzed chemiluminescence, exciting QD luminescence *via* close-proximity resonance energy transfer; upon disassembly, the signal vanished. This work combined DNA'S precise encoding capabilities with dissipative reaction networks to achieve spatiotemporal dynamic regulation of nanoparticle assembly structures and optical functions.[128]

5.3 Others

Existing DNA surface patterning techniques struggle to achieve high-precision dynamic control, and traditional enzyme-driven rolling machines can only move randomly, lacking directional control mechanisms. Recently, Huang *et al.* developed a photoactivatable DNA/RNA interface that combines RNase H cleavage to achieve programmable directed motion from rigid particles to soft-material cellular rolling machines.[129] They modified the SiO_2 particles with cage-locked RNA hairpin structures on a gold glass surface. Ultraviolet light triggered the cage unlocking, releasing the RNA strands. The SiO_2 particles, modified with DNA strands as motile legs, bound to the interface activation site. The rolling machine hybridized with interface RNA to form DNA/RNA double strands. RNase H cleaved the RNA, allowing the rolling machine to dissociate and roll to adjacent sites. Increased light intensity boosted the SiO_2 rolling distance by 2.3 times, reaching a speed of 0.3 μm min^{-1}.

Reconfigurable mechanical response crystal materials hold significant applications. Mirkin *et al.* employed DNA-modified gold nanoparticles to self-assemble into body-centered cubic superlattices *via* complementary DNA strands.[23] With a viscoelastic volume fraction exceeding 97% and DNA bond lengths exceeding 6 nm, the crystals achieved high flexibility. Upon dehydration, the crystal exhibited irregular deformations such as wrinkles and folds. Within one second of rehydration, it recovered its initial rhombic dodecahedral morphology, maintaining structural integrity even after six cycles. This realized shape-memory functionality in crystalline materials. Furthermore, they employed a synergistic strategy combining top-down lithography with bottom-up DNA-programmed assembly to achieve large-scale construction of reconfigurable, multi-component, and multi-level nanoparticle structures on gold surfaces (Fig. 9c).[19] Leveraging the sensitivity of DNA-bonded layers to solvent polarity, they achieved reversible regulation of interlayer distances within the superlattice by altering the ethanol–water mixed solvent ratio. As the ethanol proportion increased from 0% to 80%, the average absorption efficiency of the superlattice for light wavelengths between 550 and 800 nm rose by 75%.

Combining split aptamers with nanozymes enables highly sensitive detection of target molecules. Wang *et al.* reported a colorimetric aptamer sensor based on split aptamers and DNA self-assembled four-way junction (4WJ) structures for the simultaneous detection of enrofloxacin (ENR) and ciprofloxacin (CIP).[130] The study pioneered a rational design strategy for high-affinity, group-specific split aptamers. By identifying and cleaving their key binding domains, the affinity of the split fragments was significantly enhanced. Furthermore, the split aptamer was assembled with an auxiliary DNA strand into a stable 4WJ structure. A composite nanozyme composed of chitin oligosaccharide (COS)-modified AuNPs was constructed for signal output. In the presence of targets, the sensor triggered 4WJ formation,

altering the binding state between COS and AuNPs. This regulated its peroxidase-like activity, enabling visual detection.

Conclusions

In this review, we begin with nanoparticles, summarizing their synthesis methods, ligand classification, assembly techniques, and applications of DNA-mediated assemblies. Since DNA was first employed for nanoparticle assembly and construction of assemblies approximately three decades ago, this field has advanced rapidly. In the early days, DNA assembly was confined to oligomers and primarily relied on the interactions between DNA strands. Predictable structures could be assembled by manipulating the DNA strands and nanoparticles. Significant progress was achieved with the emergence of DNA tiles and DNA origami. Theoretically, by loading nanoparticles onto DNA origami structures, it is possible to position nanoparticles almost anywhere desired, which is the foundation of DNA assemblies with great potential for application. To achieve assembled structures with specific functions, obtaining nanoparticles with corresponding properties is the first step. Nanoparticle synthesis primarily originated in the past century, during which researchers proposed numerous classical methods such as the Turkevich method and the Brust–Schiffrin method. However, many of these classical synthesis methods face significant environmental challenges. In recent years, green synthesis methods emerged as a new trend. By harnessing the potential of biological resources including plant extracts and microorganisms that act as both reducing agents and stabilizers, these methods are highly environmentally friendly, energy-efficient, and simple to implement. However, despite their clear advantages, biological extracts are influenced by factors like seasonality and origin, making them less controllable than traditional methods. Furthermore, the mechanisms underlying most green synthesis approaches remain unclear. Therefore, a thorough understanding of the action mechanisms of biological extracts may significantly enhance the controls over nanoparticle size and morphology. On the other hand, the morphology of nanoparticles significantly influences their properties, which many synthetic methods struggle to precisely control. DNA-mediated synthesis enables the construction of morphologically designed DNA templates, allowing nanoparticles to grow within these templates and yield corresponding morphologies. Nevertheless, nanoparticles synthesized using DNA templates are consistently encapsulated within the DNA structure. The challenges of producing particles with specific shapes on a large scale and subsequently detaching them from the DNA to enable binding with new ligands have yet to be addressed. In the preceding review, we thoroughly discussed the DNA-mediated assembly that is highly mature for superlattice construction. By adjusting DNA strands, salt concentrations, and external catalysts, diverse lattice structures can be achieved, even customizing low-dimensional and high-dimensional defects. Researchers summarized the effects of these factors on lattice structures and mapped phase diagrams. Recently, research in this field increasingly integrated artificial intelligence and machine learning. Numerous advanced algorithms and designs emerged, such as inverse design algorithms based on two-dimensional wallpaper group symmetries, SAT optimizer designs, and the symmetry mapping algorithm MOSES. In 2011, Mirkin *et al.* proposed six design rules for constructing DNA-modified nanoparticle lattices and successfully assembled nine lattice structures. These lattice structures emerged as thermodynamically and kinetically stable outcomes under varying conditions. However, obtaining crystal structures not previously assembled or not covered by the six rules may require multiple iterations of assembling under different conditions. Inverse design approaches can skip these exploratory steps, enabling direct assembly toward the desired outcome. Therefore, inverse design represents a significant future development trend.

Although DNA-mediated nanoparticle assembly techniques have reached considerable maturity, most research remains confined to the laboratory stage. Transforming the synthesis of DNA assemblies from experimental procedures into industrial processes demands significant time and equipment costs. Superlattice construction requires slow annealing in precisely temperature-controlled equipment, typically taking a week or several weeks. Decoupling the synthesis environment from the annealing conditions and allowing the process to be conducted under conventional settings, such as ambient temperature, represents a promising approach to synthesis. This strategy has the potential to overcome the limitations imposed by restricted instrument space on product yield and to decrease overall synthesis costs. In recent work by the Tian group, urea was used as a catalyst to achieve efficient synthesis of DNA origami single crystals at room temperature. This provides crucial insights for large-scale production of DNA assemblies, demonstrating that DNA production can be scaled up through the regulation of exogenous catalysts. Following the formation of the assemblies, it is prone to disintegration or collapse as a result of environmental influences, thereby necessitating the development of methods for long-term preservation. Inorganic encapsulation of DNA origami has been proposed as a potential approach; however, this method is irreversible and precludes the functional utilization of the DNA strands themselves. The application of certain biodegradable encapsulation materials may hold considerable promise, particularly in the context of DNA information reproduction and related fields.

In nanoparticle assemblies, the properties of the nanoparticles determine the performance of the final product. DNA assembly techniques are well established for constructing superlattices of nanoparticles such as gold and silver. However, research on the assembly of a broader range

of nanomaterials remains limited. The Mirkin group extended the assembly of nanoparticles like quantum dots and platinum using azide–alkyne cycloaddition reactions. This approach provides a viable DNA modification pathway for any hydrophobic nanoparticle. Moving forward, extending DNA-mediated assembly strategies to broader nanomaterial systems represents both an inevitable trend and new challenges: (1) the membrane fluidity and deformability of soft nanoparticles enable the construction of dynamically responsive drug delivery carriers or artificial cellular networks. Achieving robust and directional DNA anchoring on their flexible surfaces while maintaining structural integrity remains an urgent research priority; (2) DNA assembly provides nanoscale alignment and programmable spacing for heterojunctions between nanowires/QDs and plasmonic–semiconductor coupling, enabling device-relevant interface energy level/barrier engineering. However, precise band alignment, interface traps, barriers caused by organic ligands, and DNA stability during post-processing remain core challenges; (3) integrating protein catalytic and recognition functions with DNA's precise spatial orchestration enables construction of efficient bioreactors and sensor arrays. Key challenges include achieving chemically orthogonal linkages while preserving conformation and activity, mitigating crowding effects, and addressing uncertainties arising from dynamic flexibility.

In recent years, significant progress has been made in the array integration of DNA crystals on substrates, enabling the patterned distribution and millimeter-level-organized assembly of DNA origami crystals. However, several challenges require further resolution: (1) addressable patterning and alignment on substrates remain fragile, strongly coupled to substrate surface chemistry and ionic environments, resulting in insufficient yield and reproducibility; (2) DNA frameworks exhibit poor tolerance to lithography, etching, and deposition, which necessitated prior inorganic conversion like silicification. However, the silicification process still faces a deficiency in coating uniformity and connectivity. Achieving integrated and device-scale DNA assemblies requires cross-disciplinary researchers to establish a reusable, quantifiable process chain. Advancing the integration of functional superlattices necessitates a theoretical examination of the coupling interactions between array patterns and DNA superlattice architectures, thereby achieving the tailored design of DNA crystal devices to fulfill specific functional criteria. Moreover, the inherently low electrical conductivity of DNA poses significant challenges for functionalization. The application of coatings composed of highly conductive materials presents a promising strategy to address this limitation. Nonetheless, such mineralization of DNA origami structures tends to compromise the nanoscale resolution of the DNA framework. Consequently, preserving high-resolution structural integrity within micrometer-scale crystals under dehydrated conditions remains a critical and unresolved challenge.

In the future, a viable fabrication process for nanoparticle devices may involve an inverse-engineering approach grounded in the application-specific requirements. Initially, the structure and composition of the nanoparticle superlattice are designed based on required functions; subsequently, targeted synthesis and functionalization of the nanoparticles are performed; finally, the individual components are assembled and integrated in accordance with the predetermined design specifications. This systematic design and manufacturing methodology holds the potential to enable the customization and intelligent development of nanoparticle-based devices while also offering a more accessible and cost-effective technological pathway for future advancements in material design.

Author contributions

Conceptualization and supervision: L. H., Y. Y., and Y. T. Investigation and methodology: L. H. and Y. Y. Visualization and writing – original draft: L. H. Writing – review and editing: L. H., Y. Y., P. L., and Y. T. Supervision and validation: Y. Y. and Y. T.

Conflicts of interest

There are no conflicts to declare.

Data availability

No primary research results, software or code have been included and no new data were generated or analysed as part of this review.

Acknowledgements

This work is supported by the National Natural Science Foundation of China (Grant No. 22372077, Grant No. 92356304).

References

1 J. A. Scholl, A. L. Koh and J. A. Dionne, *Nature*, 2012, **483**, 421–427.
2 Q. Zhang, W. Li, C. Moran, J. Zeng, J. Chen, L.-P. Wen and Y. Xia, *J. Am. Chem. Soc.*, 2010, **132**, 11372–11378.
3 J. F. Li, Y. F. Huang, Y. Ding, Z. L. Yang, S. B. Li, X. S. Zhou, F. R. Fan, W. Zhang, Z. Y. Zhou, D. Y. Wu, B. Ren, Z. L. Wang and Z. Q. Tian, *Nature*, 2010, **464**, 392–395.
4 M. Rey, A. D. Law, D. M. A. Buzza and N. Vogel, *J. Am. Chem. Soc.*, 2017, **139**, 17464–17473.
5 W. M. Park and J. A. Champion, *ACS Nano*, 2016, **10**, 8271–8280.
6 Z. Wang, Z. Li and Z. Liu, *J. Phys. Chem. C*, 2009, **113**, 3899–3902.
7 Y. Zhou, R. L. Marson, G. van Anders, J. Zhu, G. Ma, P. Ercius, K. Sun, B. Yeom, S. C. Glotzer and N. A. Kotov, *ACS Nano*, 2016, **10**, 3248–3256.

8 P. W. K. Rothemund, *Nature*, 2006, **440**, 297–302.
9 H. Liu, M. Matthies, J. Russo, L. Rovigatti, R. P. Narayanan, T. Diep, D. McKeen, O. Gang, N. Stephanopoulos, F. Sciortino, H. Yan, F. Romano and P. Šulc, *Science*, 2024, **384**, 776–781.
10 J. S. Kahn, B. Minevich, A. Michelson, H. Emamy, J. Wu, H. Ji, A. Yun, K. Kisslinger, S. Xiang, N. Yu, S. K. Kumar and O. Gang, *Nat. Mater.*, 2025, **24**, 1273–1282.
11 H. Liang, W. Wang, Y. Huang, S. Zhang, H. Wei and H. Xu, *J. Phys. Chem. C*, 2010, **114**, 7427–7431.
12 D. Pratolongo, M. Campolucci, M. Vocciante, L. Pugliesi, E. Di Giorgio, C. Lambruschini, L. Manna and F. Locardi, *Small*, 2025, 2500535.
13 J. Ye, O. Aftenieva, T. Bayrak, A. Jain, T. A. F. König, A. Erbe and R. Seidel, *Adv. Mater.*, 2021, **33**, 2100381.
14 K. De Nolf, S. M. Cosseddu, J. J. Jasieniak, E. Drijvers, J. C. Martins, I. Infante and Z. Hens, *J. Am. Chem. Soc.*, 2017, **139**, 3456–3464.
15 M. V. Kovalenko, M. Scheele and D. V. Talapin, *Science*, 2009, **324**, 1417–1420.
16 J. I. Cutler, D. Zheng, X. Xu, D. A. Giljohann and C. A. Mirkin, *Nano Lett.*, 2010, **10**, 1477–1480.
17 J.-S. Lee, A. K. R. Lytton-Jean, S. J. Hurst and C. A. Mirkin, *Nano Lett.*, 2007, **7**, 2112–2115.
18 S. Wang, S. S. Park, C. T. Buru, H. Lin, P.-C. Chen, E. W. Roth, O. K. Farha and C. A. Mirkin, *Nat. Commun.*, 2020, **11**, 2495.
19 Q.-Y. Lin, J. A. Mason, Z. Li, W. Zhou, M. N. O'Brien, K. A. Brown, M. R. Jones, S. Butun, B. Lee, V. P. Dravid, K. Aydin and C. A. Mirkin, *Science*, 2018, **359**, 669–672.
20 Y. Tian, J. R. Lhermitte, L. Bai, T. Vo, H. L. Xin, H. Li, R. Li, M. Fukuto, K. G. Yager, J. S. Kahn, Y. Xiong, B. Minevich, S. K. Kumar and O. Gang, *Nat. Mater.*, 2020, **19**, 789–796.
21 L. Dai, X. Hu, M. Ji, N. Ma, H. Xing, J.-J. Zhu, Q. Min and Y. Tian, *Proc. Natl. Acad. Sci. U. S. A.*, 2023, **120**, e2302142120.
22 K. Martens, T. Funck, E. Y. Santiago, A. O. Govorov, S. Burger and T. Liedl, *ACS Nano*, 2022, **16**, 16143–16149.
23 S. Lee, H. A. Calcaterra, S. Lee, W. Hadibrata, B. Lee, E. Oh, K. Aydin, S. C. Glotzer and C. A. Mirkin, *Nature*, 2022, **610**, 674–679.
24 J. Turkevich, P. C. Stevenson and J. Hillier, *Discuss. Faraday Soc.*, 1951, **11**, 55.
25 M. Brust, M. Walker, D. Bethell, D. J. Schiffrin and R. Whyman, *J. Chem. Soc., Chem. Commun.*, 1994, 801–802.
26 P. C. Lee and D. Meisel, *J. Phys. Chem.*, 1982, **86**, 3391–3395.
27 M. Zhou, C. Li and J. Fang, *Chem. Rev.*, 2021, **121**, 736–795.
28 Y. Liu, M. Chi, V. Mazumder, K. L. More, S. Soled, J. D. Henao and S. Sun, *Chem. Mater.*, 2011, **23**, 4199–4203.
29 D. Chatterjee, S. Shetty, K. Müller-Caspary, T. Grieb, F. F. Krause, M. Schowalter, A. Rosenauer and N. Ravishankar, *Nano Lett.*, 2018, **18**, 1903–1907.
30 Z. Wang, X. Yao, Y. Kang, L. Miao, D. Xia and L. Gan, *Adv. Funct. Mater.*, 2019, **29**, 1902987.
31 M. Luo, Z. Zhao, Y. Zhang, Y. Sun, Y. Xing, F. Lv, Y. Yang, X. Zhang, S. Hwang, Y. Qin, J.-Y. Ma, F. Lin, D. Su, G. Lu and S. Guo, *Nature*, 2019, **574**, 81–85.
32 N. Naimi-Shamel, P. Pourali and S. Dolatabadi, *J. Mycol. Med.*, 2019, **29**, 7–13.
33 M. Naseer, U. Aslam, B. Khalid and B. Chen, *Sci. Rep.*, 2020, **10**, 9055.
34 X. Luo, C. Lachance-Brais, A. Bantle and H. F. Sleiman, *Chem. Sci.*, 2020, **11**, 4911–4921.
35 N. H. Cho, Y. B. Kim, Y. Y. Lee, S. W. Im, R. M. Kim, J. W. Kim, S. D. Namgung, H.-E. Lee, H. Kim, J. H. Han, H. W. Chung, Y. H. Lee, J. W. Han and K. T. Nam, *Nat. Commun.*, 2022, **13**, 3831.
36 T. Mustapha, N. Misni, N. R. Ithnin, A. M. Daskum and N. Z. Unyah, *Int. J. Environ. Res. Public Health*, 2022, **19**, 674.
37 S. Jain and M. S. Mehata, *Sci. Rep.*, 2017, **7**, 15867.
38 M. Khatun, Z. Khatun, Md. R. Karim, Md. R. Habib, Md. H. Rahman and Md. A. Aziz, *Food Chem. Adv.*, 2023, **3**, 100386.
39 S. Chatterjee, J. Ramamurthy and R. Shanmugam, *Cureus*, 2023, **15**, e46088.
40 A. C. Dhanemozhi, V. Rajeswari and S. Sathyajothi, *Mater. Today: Proc.*, 2017, **4**, 660–667.
41 B. K. Juluri, Y. B. Zheng, D. Ahmed, L. Jensen and T. J. Huang, *J. Phys. Chem. C*, 2008, **112**, 7309–7317.
42 L. H. Tan, Y. Yue, N. S. R. Satyavolu, A. S. Ali, Z. Wang, Y. Wu and Y. Lu, *J. Am. Chem. Soc.*, 2015, **137**, 14456–14464.
43 N. S. R. Satyavolu, L. H. Tan and Y. Lu, *J. Am. Chem. Soc.*, 2016, **138**, 16542–16548.
44 J. J. Calvin, A. S. Brewer and A. P. Alivisatos, *Nat. Synth.*, 2022, **1**, 127–137.
45 H. Lee, D.-E. Yoon, S. Koh, M. S. Kang, J. Lim and D. C. Lee, *Chem. Sci.*, 2020, **11**, 2318–2329.
46 J. P. Koski and A. L. Frischknecht, *ACS Nano*, 2018, **12**, 1664–1672.
47 C. A. Mirkin, R. L. Letsinger and R. C. Mucic, *Nature*, 1996, **382**, 607.
48 X. Zhang, M. R. Servos and J. Liu, *J. Am. Chem. Soc.*, 2012, **134**, 7266–7269.
49 N. Killilea, M. Wu, M. Sytnyk, A. A. Yousefi Amin, O. Mashkov, E. Spiecker and W. Heiss, *Adv. Funct. Mater.*, 2019, **29**, 1807964.
50 A. P. Alivisatos, K. P. Johnssont, X. Peng, T. E. Wilsont, C. J. Loweth, M. P. Bruchez and P. G. Schultzt, *Nature*, 1996, **382**, 609.
51 B. Liu and J. Liu, *J. Am. Chem. Soc.*, 2017, **139**, 9471–9474.
52 S. Freko, M. Nikić, L. J. K. Weiß and B. Wolfrum, *Adv. Mater. Interfaces*, 2025, **12**, 2400869.
53 A. Fu, C. M. Micheel, J. Cha, H. Chang, H. Yang and A. P. Alivisatos, *J. Am. Chem. Soc.*, 2004, **126**, 10832–10833.
54 J. Zito and I. Infante, *Acc. Chem. Res.*, 2021, **54**, 1555–1564.
55 C. A. Mirkin and S. H. Petrosko, *ACS Nano*, 2023, **17**, 16291–16307.
56 H. Han, S. Kallakuri, Y. Yao, C. B. Williamson, D. R. Nevers, B. H. Savitzky, R. S. Skye, M. Xu, O. Voznyy, J.

Dshemuchadse, L. F. Kourkoutis, S. J. Weinstein, T. Hanrath and R. D. Robinson, *Nat. Mater.*, 2022, **21**, 518–525.
57 Z. Li, Q. Fan and Y. Yin, *Chem. Rev.*, 2022, **122**, 4976–5067.
58 M. R. Jones, N. C. Seeman and C. A. Mirkin, *Science*, 2015, **347**, 1260901.
59 D. Samanta, W. Zhou, S. B. Ebrahimi, S. H. Petrosko and C. A. Mirkin, *Adv. Mater.*, 2022, **34**, 2107875.
60 Q. Yang, X. Chang, J. Y. Lee, M. Saji and F. Zhang, *Nat. Commun.*, 2023, **14**, 7675.
61 H. Yan, S. H. Park, G. Finkelstein, J. H. Reif and T. H. LaBean, *Science*, 2003, **301**, 1882–1884.
62 R. Veneziano, S. Ratanalert, K. Zhang, F. Zhang, H. Yan, W. Chiu and M. Bathe, *Science*, 2016, **352**, 1534–1534.
63 J. I. Cutler, E. Auyeung and C. A. Mirkin, *J. Am. Chem. Soc.*, 2012, **134**, 1376–1391.
64 O. C. Farokhzad and R. Langer, *Adv. Drug Delivery Rev.*, 2006, **58**, 1456–1459.
65 J.-M. Nam, C. S. Thaxton and C. A. Mirkin, *Science*, 2003, **301**, 1884–1886.
66 D. S. Seferos, D. A. Giljohann, H. D. Hill, A. E. Prigodich and C. A. Mirkin, *J. Am. Chem. Soc.*, 2007, **129**, 15477–15479.
67 D. A. Morrow, B. M. Scirica, K. A. A. Fox, G. Berman, J. Strony, E. Veltri, M. P. Bonaca, P. Fish, C. H. McCabe and E. Braunwald, *Am. Heart J.*, 2009, **158**, 335–341.e3.
68 S. S. Park, Z. J. Urbach, C. A. Brisbois, K. A. Parker, B. E. Partridge, T. Oh, V. P. Dravid, M. Olvera De La Cruz and C. A. Mirkin, *Adv. Mater.*, 2020, **32**, 1906626.
69 J. Zhang, D. Yao, W. Hua, J. Jin and W. Jiang, *Nano Lett.*, 2024, **24**, 13965–13971.
70 J. Zhu, H. Lin, Y. Kim, M. Yang, K. Skakuj, J. S. Du, B. Lee, G. C. Schatz, R. P. Van Duyne and C. A. Mirkin, *Adv. Mater.*, 2020, **32**, 1906600.
71 N. S. Chellam, H. A. Calcaterra, Q. Xiong, G. C. Schatz and C. A. Mirkin, *ACS Nano*, 2025, **19**, 6520–6528.
72 I.-S. Jo, J. S. Oh, M. Soula, M. Lee, D. J. Pine, E. Ducrot and G.-R. Yi, *Chem. Mater.*, 2024, **36**, 3820–3828.
73 J.-L. Mergny and D. Sen, *Chem. Rev.*, 2019, **119**, 6290–6325.
74 J. Dong, M. P. O'Hagan and I. Willner, *Chem. Soc. Rev.*, 2022, **51**, 7631–7661.
75 L. Hu, X. Liu, A. Cecconello and I. Willner, *Nano Lett.*, 2014, **14**, 6030–6035.
76 Y. Ouyang, P. Zhang, H. Manis-Levy, Y. Paltiel and I. Willner, *J. Am. Chem. Soc.*, 2021, **143**, 17622–17632.
77 H. Yu, O. Alkhamis, J. Canoura, Y. Liu and Y. Xiao, *Angew. Chem., Int. Ed.*, 2021, **60**, 16800–16823.
78 Y. Zhao, S. Ong, Y. Chen, P.-J. Jimmy Huang and J. Liu, *Anal. Chem.*, 2022, **94**, 10175–10182.
79 X. Wang, K. Huang, N. Cheng and J. Liu, *Biosens. Bioelectron.*, 2025, **289**, 117863.
80 X. Wang, K. Huang, N. Cheng and J. Liu, *Biosens. Bioelectron.*, 2025, **289**, 117863.
81 W. Zhou, Y. Li, K. Je, T. Vo, H. Lin, B. E. Partridge, Z. Huang, S. C. Glotzer and C. A. Mirkin, *Science*, 2024, **383**, 312–319.
82 W. Zhou, Y. Lim, H. Lin, S. Lee, Y. Li, Z. Huang, J. S. Du, B. Lee, S. Wang, A. Sánchez-Iglesias, M. Grzelczak, L. M. Liz-Marzán, S. C. Glotzer and C. A. Mirkin, *Nat. Mater.*, 2024, **23**, 424–428.
83 M. N. O'Brien, M. Girard, H.-X. Lin, J. A. Millan, M. Olvera de la Cruz, B. Lee and C. A. Mirkin, *Proc. Natl. Acad. Sci. U. S. A.*, 2016, **113**, 10485–10490.
84 M. R. Jones, R. J. Macfarlane, B. Lee, J. Zhang, K. L. Young, A. J. Senesi and C. A. Mirkin, *Nat. Mater.*, 2010, **9**, 913–917.
85 H. A. Calcaterra, N. S. Chellam, B. Lee, G. C. Schatz and C. A. Mirkin, *ACS Nano*, 2024, **18**, 28268–28278.
86 M. R. Begley, D. S. Gianola and T. R. Ray, *Science*, 2019, **364**, eaav4299.
87 K. R. Phillips, G. T. England, S. Sunny, E. Shirman, T. Shirman, N. Vogel and J. Aizenberg, *Chem. Soc. Rev.*, 2016, **45**, 281–322.
88 M. Liu, X. Zheng, V. Grebe, M. He, D. J. Pine and M. Weck, *Angew. Chem., Int. Ed.*, 2021, **60**, 5744–5748.
89 Z. Miao, C. Y. Zheng, G. C. Schatz, B. Lee and C. A. Mirkin, *Angew. Chem., Int. Ed.*, 2021, **60**, 19035–19040.
90 Z. Li, Y. Lim, I. Tanriover, W. Zhou, Y. Li, Y. Zhang, K. Aydin, S. C. Glotzer and C. A. Mirkin, *Sci. Adv.*, 2024, **10**, eadp3756.
91 Y. Li, W. Zhou, I. Tanriover, W. Hadibrata, B. E. Partridge, H. Lin, X. Hu, B. Lee, J. Liu, V. P. Dravid, K. Aydin and C. A. Mirkin, *Nature*, 2022, **611**, 695–701.
92 F. Zhang, J. Nangreave, Y. Liu and H. Yan, *J. Am. Chem. Soc.*, 2014, **136**, 11198–11211.
93 E. Winfree, F. Liu, L. A. Wenzler and N. C. Seeman, *Nature*, 1998, **394**, 539–544.
94 Y. Zhang, D. Yang, P. Wang and Y. Ke, *ACS Nano*, 2023, **17**, 10486–10495.
95 R. Wu, Y. Chen, Y. Zhang, R. Liu, Q. Zhang and C. Zhang, *Small*, 2024, **20**, 2307107.
96 J. R. Burns, *Small*, 2021, **17**, 2100136.
97 Y. Tian, T. Wang, W. Liu, H. L. Xin, H. Li, Y. Ke, W. M. Shih and O. Gang, *Nat. Nanotechnol.*, 2015, **10**, 637–644.
98 Y. Tian, Y. Zhang, T. Wang, H. L. Xin, H. Li and O. Gang, *Nat. Mater.*, 2016, **15**, 654–661.
99 Y. Dong, J. Liu, X. Lu, J. Duan, L. Zhou, L. Dai, M. Ji, N. Ma, Y. Wang, P. Wang, J.-J. Zhu, Q. Min, O. Gang and Y. Tian, *Nano Lett.*, 2022, **22**, 3809–3817.
100 Y. Yu, M. Ji, Y. Wang, X. Yan, L. Dai, N. Ma, Z. Zhou, H. Xing and Y. Tian, *Chem. Sci.*, 2025, **16**, 793–801.
101 Y. Wang, X. Yan, Z. Zhou, N. Ma and Y. Tian, *Angew. Chem., Int. Ed.*, 2022, **61**, e202208290.
102 N. Ma, L. Dai, Z. Chen, M. Ji, Y. Wang and Y. Tian, *Nano Lett.*, 2021, **21**, 3581–3587.
103 L. Ding, W. Ma, X. Chen, H. Wang, H. Song, C. Fan, X. Liu and G. Yao, *Angew. Chem., Int. Ed.*, 2025, **64**, e202424230.
104 K. Martens, F. Binkowski, L. Nguyen, L. Hu, A. O. Govorov, S. Burger and T. Liedl, *Nat. Commun.*, 2021, **12**, 2025.

105 Y. Li, J. Pei, X. Lu, Y. Jiao, F. Liu, X. Wu, J. Liu and B. Ding, *J. Am. Chem. Soc.*, 2021, **143**, 19893–19900.
106 S. Yang, W. Liu, Y. Zhang and R. Wang, *ACS Appl. Mater. Interfaces*, 2021, **13**, 50516–50523.
107 S. Huang, M. Ji, Y. Wang and Y. Tian, *Chem. Sci.*, 2023, **14**, 11507–11514.
108 F. Romano, *Phys. Rev. Lett.*, 2020, **125**, 118003.
109 S. Whitelam and I. Tamblyn, *Phys. Rev. E*, 2020, **101**, 52604.
110 S. Adhikari, B. Minevich, D. Redeker, A. N. Michelson, H. Emamy, E. Shen, O. Gang and S. K. Kumar, *J. Am. Chem. Soc.*, 2023, **145**, 19578–19587.
111 D. Hayakawa, T. E. Videbæk, G. M. Grason and W. B. Rogers, *ACS Nano*, 2024, **18**, 19169–19178.
112 J. S. Kahn, D. C. Redeker, A. Michelson, A. Tkachenko, S. Hong, B. Minevich and O. Gang, *ACS Nano*, 2025, **19**, 14795–14807.
113 Y. Fan, J. Ma, Y. Li, X. Huang, S. Feng and D. Chen, *Chem. Mater.*, 2024, **36**, 4011–4033.
114 Y. Yamada, C.-K. Tsung, W. Huang, Z. Huo, S. E. Habas, T. Soejima, C. E. Aliaga, G. A. Somorjai and P. Yang, *Nat. Chem.*, 2011, **3**, 372–376.
115 E. Auyeung, W. Morris, J. E. Mondloch, J. T. Hupp, O. K. Farha and C. A. Mirkin, *J. Am. Chem. Soc.*, 2015, **137**, 1658–1662.
116 E. Auyeung, W. Morris, J. E. Mondloch, J. T. Hupp, O. K. Farha and C. A. Mirkin, *J. Am. Chem. Soc.*, 2015, **137**, 1658–1662.
117 M. S. Hizir, M. Top, M. Balcioglu, M. Rana, N. M. Robertson, F. Shen, J. Sheng and M. V. Yigit, *Anal. Chem.*, 2016, **88**, 600–605.
118 C. Zeng, N. Lu, Y. Wen, G. Liu, R. Zhang, J. Zhang, F. Wang, X. Liu, Q. Li, Z. Tang and M. Zhang, *ACS Appl. Mater. Interfaces*, 2019, **11**, 1790–1799.
119 W. Mei, W. Huang, X. Liu, H. Wang, Q. Wang, X. Yang and K. Wang, *Anal. Chem.*, 2023, **95**, 11391–11398.
120 J. Xiao, X. Yang, X. Zhang, X. Niu, Y. Guo, N. Zhu, K. Zeng and Z. Zhang, *Anal. Chem.*, 2024, **96**, 19796–19802.
121 M. Cai, Y. Zhang, Z. Cao, W. Lin and N. Lu, *ACS Appl. Mater. Interfaces*, 2023, **15**, 18620–18629.
122 A. Kuzyk, R. Schreiber, Z. Fan, G. Pardatscher, E.-M. Roller, A. Högele, F. C. Simmel, A. O. Govorov and T. Liedl, *Nature*, 2012, **483**, 311–314.
123 Y. Zhang, D. D. Xu, I. Tanriover, W. Zhou, Y. Li, R. López-Arteaga, K. Aydin and C. A. Mirkin, *Nat. Photonics*, 2025, **19**, 20–27.
124 J. Zhang, C. Song, X. He, J. Liu, J. Chao and L. Wang, *Chem. Soc. Rev.*, 2025, **54**, 5836–5863.
125 D. Meng, W. Ma, X. Wu, C. Xu and H. Kuang, *Small*, 2020, **16**, 2000003.
126 K. Tapio, A. Mostafa, Y. Kanehira, A. Suma, A. Dutta and I. Bald, *ACS Nano*, 2021, **15**, 7065–7077.
127 R. Niu, F. Gao, D. Wang, D. Zhu, S. Su, S. Chen, L. YuWen, C. Fan, L. Wang and J. Chao, *ACS Nano*, 2022, **16**, 14622–14631.
128 Y. Ouyang, P. Zhang, H. Manis-Levy, Y. Paltiel and I. Willner, *J. Am. Chem. Soc.*, 2021, **143**, 17622–17632.
129 D. Chen, Y. Qin, S. Xu, F. Xia, I. Willner and F. Huang, *Small*, 2025, 2506270.
130 W. Wang, L. Zhang, W. Dong, K. Wei, J. Li, J. Sun, S. Wang and X. Mao, *J. Hazard. Mater.*, 2023, **458**, 131995.